


Search for pair-produced resonances decaying to quark pairs in proton-proton collisions at $\sqrt{s} = 13$ TeV

A. M. Sirunyan *et al.**
(CMS Collaboration)

 (Received 9 August 2018; published 28 December 2018)

A general search for the pair production of resonances, each decaying to two quarks, is reported. The search is conducted separately for heavier resonances (masses above 400 GeV), where each of the four final-state quarks generates a hadronic jet resulting in a four-jet signature, and for lighter resonances (masses between 80 and 400 GeV), where the pair of quarks from each resonance is collimated and reconstructed as a single jet resulting in a two-jet signature. In addition, a b -tagged selection is applied to target resonances with a bottom quark in the final state. The analysis uses data collected with the CMS detector at the CERN LHC, corresponding to an integrated luminosity of 35.9 fb^{-1} , from proton-proton collisions at a center-of-mass energy of 13 TeV. The mass spectra are analyzed for the presence of new resonances, and are found to be consistent with standard model expectations. The results are interpreted in the framework of R -parity-violating supersymmetry assuming the pair production of scalar top quarks decaying via the hadronic coupling λ''_{312} or λ''_{323} and upper limits on the cross section as a function of the top squark mass are set. These results probe a wider range of masses than previously explored at the LHC, and extend the top squark mass limits in the $\tilde{t} \rightarrow qq'$ scenario.

DOI: [10.1103/PhysRevD.98.112014](https://doi.org/10.1103/PhysRevD.98.112014)

I. INTRODUCTION

New particles that decay into quarks and gluons and produce fully hadronic signatures are predicted in many models of physics beyond the standard model (SM) [1–3]. For instance, the violation of baryon number in certain supersymmetric (SUSY) models leads to colored superpartners producing fully hadronic final states [4]. In this paper, we report on a generic search for pair-produced resonances decaying to two light quarks (qq') or one light quark and one bottom quark (bq').

Minimal SUSY models introduce R -parity, associated with a Z_2 symmetry group called R symmetry, to forbid terms in the SUSY potential that naturally lead to the violation of baryon or lepton numbers [5]. After SUSY breaking, R -parity violating Yukawa interactions of the form

$$\lambda_{ijk} L_i L_j E_k^c, \quad \lambda'_{ijk} L_i Q_j D_k^c, \quad \lambda''_{ijk} U_i^c D_j^c D_k^c, \quad (1)$$

can appear in the Lagrangian, where λ , λ' , λ'' are coupling constants, and i, j, k are quark and lepton generation indices following the summation convention, while c denotes

charge conjugation. The $SU(2)$ doublet superfields of the lepton and quark are denoted by L_i and Q_i , respectively, while the E_i , U_i and, D_j represent the $SU(2)$ singlet superfields of the lepton, up- and down-type quarks, respectively. The first and third terms in Eq. (1) are antisymmetric in $\{i, j\}$ and $\{j, k\}$, respectively. The trilinear couplings λ''_{ijk} permit vertices of sfermions interacting with two fermions, and in baryonic R -parity-violating (RPV) models, the only nonzero couplings in Eq. (1) are λ''_{ijk} , which produce interactions of squarks with two quarks.

We consider pair production of top squarks (\tilde{t}) as a benchmark model, assuming the \tilde{t} is the lightest of the colored SUSY partners and is allowed to decay via the baryonic RPV coupling to quarks. In this case $\lambda''_{ijk} = \lambda''_{3DD}$ and each index reflects the squark or quark generation of the process, two of which are down-type quarks. Two possible choices of hadronic RPV coupling scenarios are studied: $\tilde{t} \rightarrow qq'$ through the coupling λ''_{312} , and $\tilde{t} \rightarrow bq'$ through the coupling λ''_{323} . The couplings considered are assumed to be large enough such that the resulting decays are prompt. These two models are schematically depicted in Fig. 1.

Searches for $\tilde{t} \rightarrow qq'$ via RPV decays have been performed at CERN by the ALEPH experiment at LEP [6], which excluded $m_{\tilde{t}} < 80$ GeV at 95% confidence level (CL), and subsequently by the CDF experiment [7] at the Fermilab Tevatron, which extended the limit to $m_{\tilde{t}} < 100$ GeV. Similar searches have been performed at the CERN LHC by both the CMS and ATLAS experiments at center-of-mass

*Full author list given at the end of the article.

Published by the American Physical Society under the terms of the [Creative Commons Attribution 4.0 International license](https://creativecommons.org/licenses/by/4.0/). Further distribution of this work must maintain attribution to the author(s) and the published article's title, journal citation, and DOI. Funded by SCOAP³.

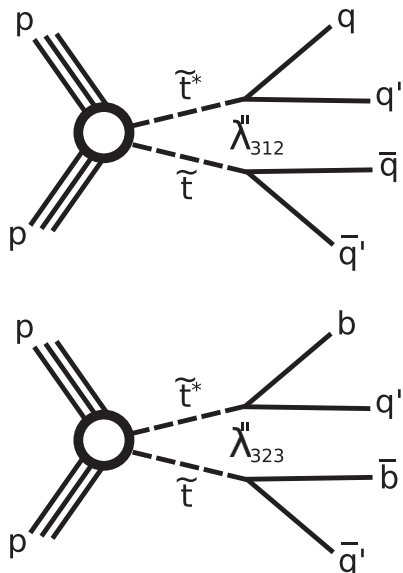


FIG. 1. Diagrams for the benchmark models used in this analysis: pair production of top squarks decaying into qq' via the RPV coupling λ''_{312} (top), and bq' via the RPV coupling λ''_{323} (bottom).

energies $\sqrt{s} = 7, 8,$ and 13 TeV; CMS [8] excluded $200 < m_{\tilde{t}} < 350$ GeV at $\sqrt{s} = 8$ TeV, while the ATLAS exclusion [9] is $100 < m_{\tilde{t}} < 410$ GeV at $\sqrt{s} = 13$ TeV. For the $\tilde{t} \rightarrow bq'$ scenario, mass exclusion limits at $\sqrt{s} = 8$ TeV have been reported by CMS [8] of $200 < m_{\tilde{t}} < 385$ GeV, and by ATLAS [10] of $100 < m_{\tilde{t}} < 310$ GeV, and at $\sqrt{s} = 13$ TeV ATLAS [9] excluded $100 < m_{\tilde{t}} < 470$ GeV and $480 < m_{\tilde{t}} < 610$ GeV.

The analysis reported in this paper uses pp collision data at $\sqrt{s} = 13$ TeV collected with the CMS detector [11] at the LHC in 2016, corresponding to an integrated luminosity of 35.9 fb^{-1} [12]. The search is conducted in two mass ranges. The mass spectrum between 60 and 450 GeV is used to search for lighter resonances between 80 and 400 GeV, where the decay products of each of the resonances are sufficiently collimated to be reconstructed as a single jet (boosted search). The mass spectrum above 350 GeV is explored for the presence of heavier resonances above 400 GeV, where four jets are reconstructed in the final state (resolved search). Together they target resonance masses between 80 and 1500 GeV. When b tagging requirements are applied to either of the searches, we refer to the selection as b tagged, and interpret the results in the $\tilde{t} \rightarrow bq'$ scenario. When no b tagging is applied, we refer to the selection as inclusive, and interpret the results in the $\tilde{t} \rightarrow qq'$ scenario. In both searches, the selection criteria and analysis strategies are general, such that any pair produced diquark resonance with a narrow width and sufficient cross section would appear as a local enhancement in the mass spectra.

The low-mass boosted search exploits the internal structure of the jets to differentiate between signal jets

(two-prong structure) and jets coming from quantum chromodynamics (QCD) multijet processes (predominantly with no internal structure). In this search, we use the average mass of the two jets with the highest transverse momentum (p_T), after removing soft and wide-angle QCD multijet radiation, to look for evidence of a signal consistent with localized deviations from the estimated SM backgrounds. The primary SM background component—QCD multijet events—is estimated from data control samples. Subdominant SM processes, such as the single and double production of W and Z bosons, and top quarks decaying hadronically, are taken into account with simulated samples. These backgrounds create resonances in the mass spectrum, and they are henceforth referred to as resonant backgrounds.

For the resolved search, the high-mass resonances are produced with insufficient boost for the decay products to be merged into single jets, and events with four individual high transverse momentum (p_T) jets are selected. The dijet mass spectrum in this search is also dominated by QCD multijet production. The mass spectrum is parametrized as a steeply falling smooth distribution that is explored for signal-like localized excesses.

II. THE CMS DETECTOR

The central feature of the CMS apparatus is a superconducting solenoid of 6 m internal diameter, providing a magnetic field of 3.8 T. Within the solenoid volume are a silicon pixel and a strip tracker, a lead tungstate crystal electromagnetic calorimeter (ECAL), and a brass and scintillator hadron calorimeter (HCAL), each composed of a barrel and two endcap sections. Forward calorimeters extend the pseudorapidity (η) coverage provided by the barrel and endcap detectors. Muons are detected in gaseous ionization chambers embedded in the steel flux-return yoke outside the solenoid. Energy deposits from hadronic jets are measured using the ECAL and HCAL. Events of interest are selected using a two-tiered trigger system [13]. A detailed description of the CMS detector, together with a definition of the coordinate system used and the relevant kinematic variables, can be found in Ref. [11].

III. SIMULATED EVENT SAMPLES

Top squark signal events are simulated using a combination of PYTHIA 8.212 [14] and MADGRAPH 5_amc@NLO 2.2.2 [15]. The calculation of the production of a pair of top squarks with up to two additional initial-state radiation jets is performed at leading order (LO) with MADGRAPH 5_amc@NLO and MLM merging [16], while PYTHIA is used for the prompt decay of each top squark to either $\tilde{t} \rightarrow qq'$ or $\tilde{t} \rightarrow bq'$ through the λ''_{3DD} hadronic RPV couplings. For each of the coupling models considered, all other λ''_{3DD} couplings are set to zero so that the branching fraction to the desired channel is 100%. The

PYTHIA simulation is also used for the parton showering and the fragmentation with the CUETP8M1 [17] underlying event tune. For each coupling, top squarks are generated with masses between 80 and 1500 GeV, in 20 GeV increments up to 300 GeV, in 50 GeV steps up to 1 TeV, and in 100 GeV increments thereafter. All other SUSY particle masses are set to higher values in order not to produce intermediate sparticles in the top squark production and decay. The natural width of the top squark is taken to be much smaller than the detector resolution.

Processes from QCD multijets are simulated at LO via PYTHIA using the CUETP8M1 tune [17]. The production of a hadronically decaying W or Z boson accompanied by additional jets from initial- and final-state radiation ($W \rightarrow q'\bar{q} + \text{jets}$ or $Z \rightarrow q\bar{q} + \text{jets}$) [16], and ZZ diboson [18] samples are generated with MADGRAPH 5_amc@NLO, at LO with MLM merging and at next-to-leading order (NLO) with FFX merging [18], respectively. WZ processes are generated at LO with PYTHIA, and $t\bar{t} + \text{jets}$ and WW samples are generated at NLO with POWHEG v2 [19,20]. For $W \rightarrow q'\bar{q}/Z \rightarrow q\bar{q} + \text{jets}$ events, higher-order p_T -dependent electroweak NLO corrections are applied to improve the modeling of the kinematic distributions [21–25].

Additional pp interactions in the same or adjacent bunch crossings are referred to as pileup. A number of minimum bias interactions are added to the hard interaction of all simulated samples, and the events are weighted such that the distribution of the number of pileup interactions is the same as that in the data. PYTHIA is used for the parton showering and hadronization and the simulation of the CMS detector for all samples is handled by GEANT4 [26]. All simulated samples are produced with the parton distribution functions (PDF) NNPDF3.0 [27], with the precision (LO or NLO) set by the generator used.

IV. JET RECONSTRUCTION AND SELECTION

The reconstructed vertex with the largest value of summed physics-object p_T^2 is taken to be the primary pp interaction vertex. Here the physics objects are the jets, clustered using the anti- k_T jet finding algorithm [28,29], with the tracks assigned to the vertex as inputs, and the associated missing transverse momentum, taken as the negative vector p_T sum of those jets. Particle candidates in CMS are reconstructed using a particle-flow (PF) algorithm [30], which identifies muons, electrons, photons, and neutral and charged hadrons through a combination of information from the various subdetectors. The PF candidates identified as originating from pileup are removed prior to the jet clustering [31,32]. Jets with a clustering distance parameter of 0.4 (AK4 jets) and 0.8 (AK8 jets) are used for the resolved and the boosted searches, respectively. Corrections are applied to jet energies as a function of η and p_T of the jet to account for the combined response function of the detector to reconstructed objects [32,33].

For the boosted search, jet grooming techniques are used to eliminate soft, and wide-angle QCD radiation at the periphery of the jet. Grooming improves the jet mass resolution and reduces the pileup contributions to the jet mass. Two grooming algorithms are used: trimming [34] at the trigger stage and pruning [35] at the analysis stage. The trimming technique discriminates particles within the constituents of the jet based on a dynamic p_T threshold. In pruning, the constituents of the original jet are reclustered with the same distant parameter but using a modified Cambridge-Aachen (CA) algorithm [36,37] with relative p_T and angular requirements. To discriminate between jets originating from SM background processes from those from boosted hadronic resonances, N -subjettiness variables (τ_N) [38] are used, which quantify the number of N prongs of energy inside a jet. In particular, ratios of N -subjettiness variables, $\tau_{MN} = \tau_M/\tau_N$, are found to provide better discrimination between signal and background. In this analysis, $\tau_{21} = \tau_2/\tau_1$ is used to distinguish two-prong signal-like jets and one-prong backgroundlike jets which arise from QCD multijets events at an overwhelming rate, and $\tau_{32} = \tau_3/\tau_2$ to separate two-prong jets from three-prong jets from hadronically decaying top quarks.

Jets produced by the hadronization of bottom quarks are identified with a combined secondary vertex b -tagging algorithm [39]. This algorithm uses a multivariate discriminator with inputs from information related to the secondary vertex, and a track-based lifetime measurement to differentiate between jets from bottom quarks and from light-flavor quarks and gluons. The working point of the b -tagging algorithm used in this analysis is referred to as loose, and gives an $\approx 81\%$ b tagging efficiency, a $\approx 10\%$ misidentification rate for light-quark and gluon jets, and a $\approx 40\%$ misidentification rate for charm quark jets [39].

V. BOOSTED SEARCH

A. Event selection

Events are first selected with a trigger based on the total hadronic transverse momentum in the event (H_T), defined as the scalar p_T sum of AK4 jets (H_T^{AK4}) with $p_T > 30$ GeV and $|\eta| < 2.5$. The H_T^{AK4} trigger threshold for the early data-taking period was set to 800 GeV, and raised to 900 GeV for the last 8 fb $^{-1}$ of data to enable the trigger to handle the instantaneous luminosity delivered by the LHC. Additionally, we include a logical OR of two triggers based on AK8 jets: one trigger requires an AK8 jet with $p_T > 360$ GeV and trimmed mass above 30 GeV, the other requires $H_T^{\text{AK8}} > 750$ GeV defined with AK8 jets with $p_T > 150$ GeV, and a jet with trimmed mass above 50 GeV. The selection efficiency of the chosen triggers is determined relative to unbiased samples collected with muon-based triggers. This is cross checked with other samples collected with jet based triggers, and are all found to give consistent results. The signal triggers are found to

have an efficiency greater than 98% with respect to the analysis-level selection, for events satisfying $H_T^{\text{AK8}} > 900$ GeV. In addition to satisfying the trigger conditions, selected events are required to have at least two AK8 jets with $p_T > 150$ GeV, situated in the central region of the detector with $|\eta| < 2.5$, and $H_T^{\text{AK8}} > 900$ GeV.

The boosted search assumes that the decay products of the resonance would be fully contained in a very energetic AK8 jet, and therefore we select the two most energetic AK8 jets in the event. The pruning algorithm is used to compute the mass of each of these two jets (m_{j_1} and m_{j_2}). The spectrum of the average pruned jet mass of these two jets, $\bar{m} = (m_{j_1} + m_{j_2})/2$, is examined for the presence of new physics in the mass range 60–450 GeV.

The following selection criteria are applied to reduce SM background events. These criteria were optimized by maximizing the signal significance using S/\sqrt{B} as the metric within a mass window centered at the generated $m_{\tilde{t}}$, where S and B are the number of signal and background events, respectively, from simulation. The number of events with large mass imbalance between the two signal jet candidates is reduced by selecting events with mass asymmetry, defined as $m_{\text{asym}} = |m_{j_1} - m_{j_2}|/(m_{j_1} + m_{j_2})$, below 0.1. Both jets are required to satisfy $\tau_{21} < 0.45$ and $\tau_{32} > 0.57$, to reject backgrounds from QCD multijets events and those from hadronically decaying top quarks, respectively. Jets from the signal events would be predominantly produced with similar η , compared to the widely spread QCD multijet production, and thus we require events to have an absolute value of the difference in η between the two jets: $\Delta\eta = |\eta_{j_1} - \eta_{j_2}| < 1.5$. For the b -tagged selection, both jets are required to satisfy the loose b tagging criteria described in Sec. IV. All the selection criteria are summarized in Table I (second column), and are found to be optimal for the range of masses considered in this search. The discriminating power of each of these kinematic variables is illustrated in Fig. 2 where normalized distributions between data, different simulated background components, and selected simulated signal samples are presented.

B. Signal efficiency

Figure 3 (left) shows the mass distributions for simulated signals after the inclusive selection. Similar signal mass shapes are found when applying the b -tagged selection. Additionally, the signal efficiency for the boosted search is reported in Fig. 3 (right) for both the inclusive and b -tagged selections. The fraction of $\tilde{t} \rightarrow qq'$ signal events remaining after applying the inclusive selection, relative to the total number of events generated, is 0.003% for $m_{\tilde{t}} = 80$ GeV, increases to 0.106% for $m_{\tilde{t}} = 180$ GeV, and drops again to 0.055% for $m_{\tilde{t}} = 400$ GeV because of the decrease in the production of top squarks with large Lorentz boosts at higher masses. Although the fraction of boosted resonances

TABLE I. Summary of the signal selection criteria for the boosted search (second column) and resolved search (third column). The criteria are shown for the inclusive selection and the b -tagged selection.

Selection	Boosted search	Resolved search
	$60 < \bar{m} < 450$ GeV ($80 \leq m_{\tilde{t}} < 400$ GeV)	$\bar{M} > 350$ GeV ($m_{\tilde{t}} \geq 400$ GeV)
Inclusive	AK8 jets	AK4 jets
and b -tagged	Jet $p_T > 150$ GeV Jet $ \eta < 2.5$ Number of jets ≥ 2 $H_T^{\text{AK8}} > 900$ GeV $m_{\text{asym}} < 0.1$ $\tau_{21} < 0.45$ $\tau_{32} > 0.57$ $\Delta\eta < 1.5$	Jet $p_T > 80$ GeV Jet $ \eta < 2.5$ Number of jets ≥ 4 $H_T^{\text{AK4}} > 900$ GeV $M_{\text{asym}} < 0.1$ $\Delta\eta_{\text{dijet}} < 1.0$ $\Delta > 200$ GeV
b -tagged	Two loose b -tagged jets	Two loose b -tagged jets

is higher for $m_{\tilde{t}} \lesssim 170$ GeV, the H_T and p_T trigger requirements have a considerable impact on the event selection and are the main source of the signal efficiency loss. The low signal selection efficiencies for boosted resonances are compensated by the large signal cross sections for low-mass top squarks [40,41]. The b -tagged selection presents a similar pattern, where the fraction of remaining events for $\tilde{t} \rightarrow bq'$ is 0.0009%, 0.0350%, and 0.0134% for the resonance masses $m_{\tilde{t}} = 80, 200, \text{ and } 400$ GeV, respectively.

C. Background estimate

After all the selection criteria are applied, the dominant remaining SM background is QCD multijet production. Subdominant resonant backgrounds are estimated from simulation and they include $t\bar{t} + \text{jets}$, $W \rightarrow q'\bar{q} + \text{jets}$, $Z \rightarrow q\bar{q} + \text{jets}$, and diboson (WW, ZZ, WZ) production. The normalization of $t\bar{t} + \text{jets}$, the largest resonant background, is assessed in a control region enriched in $t\bar{t}$ events by requiring $\tau_{32} < 0.57$. This criterion aims to remove one- or two-prong jets, thus enriching the sample in $t\bar{t}$. We then compare the \bar{m} spectrum between data and simulation and obtain a correction factor from a first-order polynomial fit subtracting all other backgrounds. This correction is found to be flat in \bar{m} and consistent with unity within 10%, and is used as an estimate of the systematic uncertainty associated with modeling the simulated SM events. In addition, the statistical uncertainty due to the limited number of simulated SM events in each bin is considered as a systematic uncertainty, affecting the shape of the \bar{m} distribution.

The background originating from QCD multijet events is estimated by extrapolating data in sideband regions to the signal region, using two uncorrelated variables and is referred to as the $ABCD$ method. The variables m_{asym} and $\Delta\eta$ are found to have a correlation in data and in

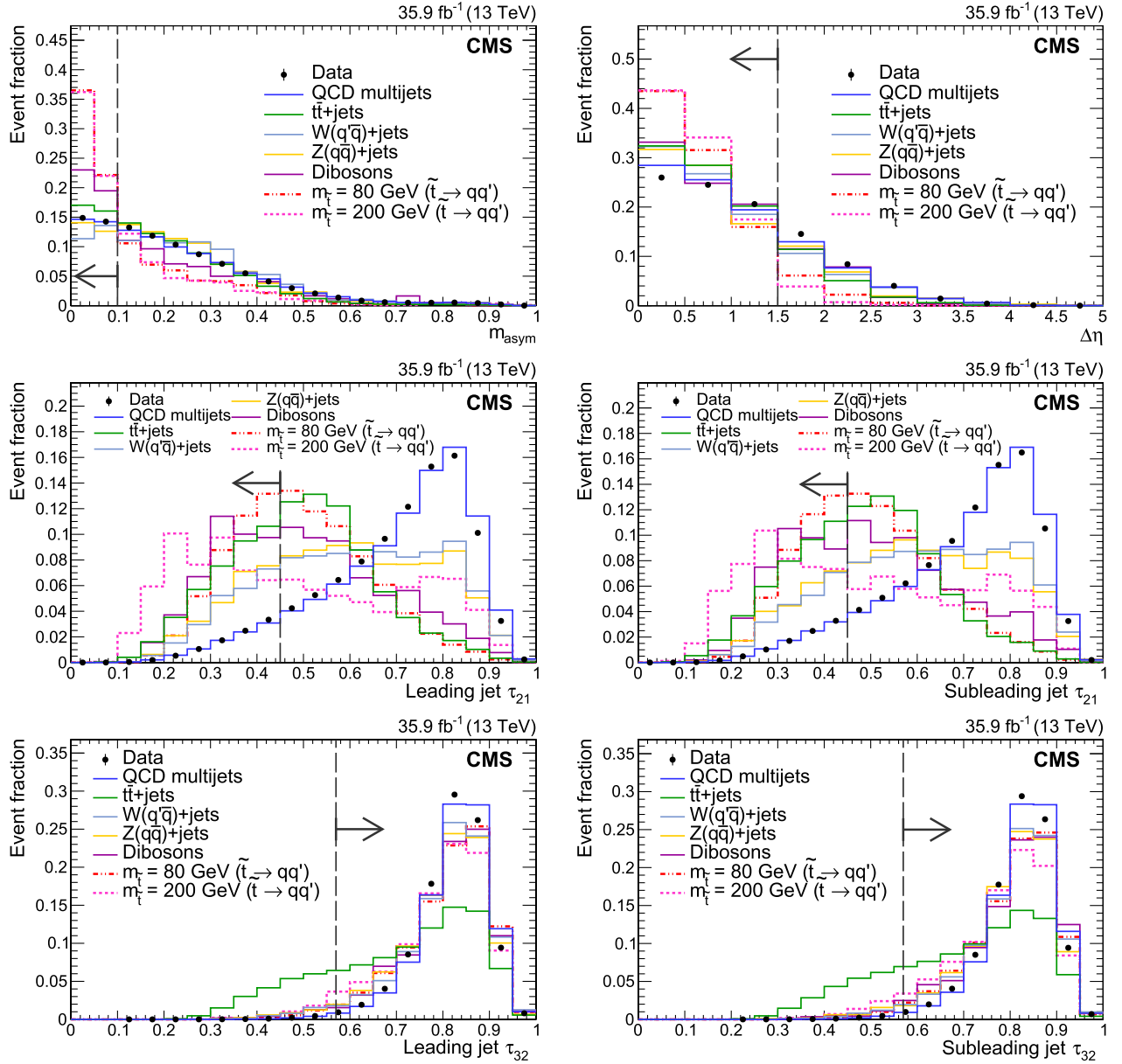


FIG. 2. Boosted search kinematic distributions, normalized to unity, showing the comparison between data (black dots), backgrounds (solid colored lines), and a few selected $\tilde{t} \rightarrow qq'$ signal simulated samples (dashed colored lines). All inclusive selection criteria are applied, apart from that on the variable being presented. In the case of the τ_{21} and τ_{32} variables, both τ_{21} and τ_{32} requirements are removed. The black dashed lines indicate the maximum value imposed by the selection in the upper and middle rows of plots, and the minimum allowed value in the lower plots. Upper left: m_{asym} . Upper right: $\Delta\eta$. Middle left: leading jet τ_{21} . Middle right: subleading jet τ_{21} . Lower left: leading jet τ_{32} . Lower right: subleading jet τ_{32} .

simulation of less than 1%, therefore, these two variables are used to define four regions summarized in Table II. Region A is the signal region defined by the nominal inclusive selection criteria, while the other three regions are background dominated. Regions B and C are sideband regions where the event must pass one of the two selection criteria and fail the other, and region D is defined as the sideband region when both selection criteria fail.

The yield and the shape of the \bar{m} spectrum for the QCD multijet background in the signal region (A) is determined

using the mass spectra in sideband regions such that $A = BC/D$. The transfer factor is defined as the ratio B/D and it is parametrized empirically as a function of \bar{m} using a sigmoid function of the form

$$f(\bar{m}) = \frac{1}{p_0 + \exp(p_1 + p_2 \bar{m}^2 - p_3 \bar{m}^3)}, \quad (2)$$

where the coefficients p_0 to p_3 are free parameters of the function. Resonant background contributions estimated

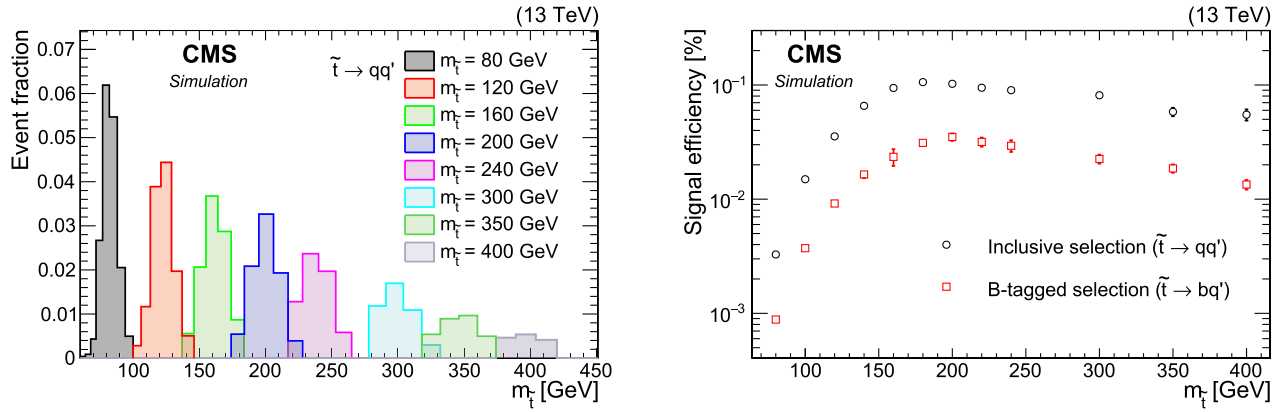


FIG. 3. Boosted search signal distributions. Left: signal mass distributions after applying the inclusive selection, for various simulated $\tilde{t} \rightarrow qq'$ masses probed in this analysis. Right: signal efficiency as a function of $m_{\tilde{t}}$ for the inclusive and b -tagged selections.

from simulation are subtracted from the data prior to the extrapolation. The fit of the transfer factor is found to give consistent results in data and simulation. The resulting fit in the data, shown in Fig. 4, is applied to events in region C to estimate the final \bar{m} distribution for QCD multijet events in region A for the inclusive selection. The uncertainty in the fitted transfer factor and the statistical uncertainty in the \bar{m} distribution in region C are treated as systematic uncertainties that affect the shape of the \bar{m} distribution.

For the b -tagged selection, an equivalent procedure is performed. Once the b tagging is applied, the data sample is found to be too small to obtain a transfer factor. Instead, the transfer factor from the inclusive selection is used, and applied to region C where the b tagging requirement is added. By comparing the fit parameters of the transfer factors obtained with the inclusive and the b -tagged selections, an additional uncertainty is applied to cover the differences, as illustrated in the dark red band of Fig. 4.

D. Systematic uncertainties

The performance of the $ABCD$ background estimate is tested on simulated QCD multijet events. In this test, the background prediction is compared to the mass spectrum in the signal region A . The level of agreement between these two distributions, or closure, is found to be within $\pm 10\%$ over the entire \bar{m} spectrum. This is used as an estimate of the contribution from this source to the systematic uncertainty in the QCD multijet background for both the inclusive and b -tagged selection.

TABLE II. Definition of the regions used in the QCD multijet background estimate for the boosted analysis. Region A is the signal-dominated region while regions B , C , and D are background-dominated sideband regions.

	$m_{\text{asym}} < 0.1$	$m_{\text{asym}} > 0.1$
$\Delta\eta > 1.5$	B	D
$\Delta\eta < 1.5$	A	C

The systematic uncertainties in the background estimates are summarized in Table III.

Systematic uncertainties affecting the expected signal yield arise from the integrated luminosity measurement (2.5%) [12], the trigger efficiency (3.0%), the modeling of the pileup interactions (1.0%), the effect from the uncertainties in the PDF (1.0%) [42], and the measurement of the jet energy scale (1.2%) and jet resolution (1.8%) [32,33]. For the b -tagged selection, the uncertainty in the efficiency for identifying bottom quarks (1.0%) contributes to the overall uncertainty in the expected signal yield [39].

Systematic uncertainties due to the jet energy scale and resolution measurements also affect the shape of the \bar{m} spectrum (independent of the yield). These uncertainties are determined using the reconstructed jet mass in hadronically decaying boosted W bosons, where differences in scale (2.0%) and resolution (14.0%) between data and simulation

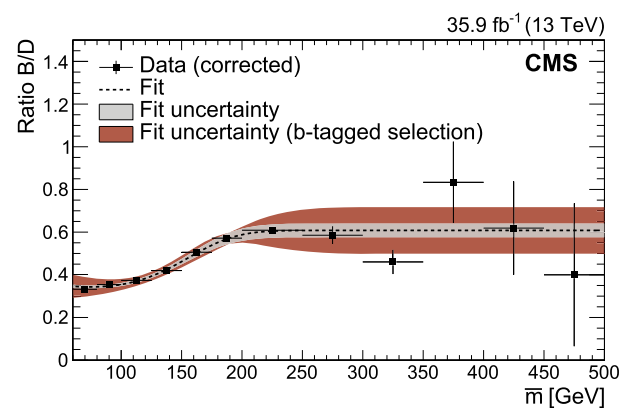


FIG. 4. Boosted search transfer factor B/D as a function of \bar{m} for data (black points) with the inclusive selection applied, and corrected for the resonant background component. The fit to the data (black dotted line) with the sigmoid function described in Eq. (2) is also displayed. Light gray and dark red bands represent the uncertainties of the fit for the inclusive and b -tagged selection, respectively, and are treated as systematic uncertainties.

TABLE III. Summary of the sources of systematic uncertainties in the background predictions. The values of the systematic uncertainties and whether they affect the overall event yield or the shape of the mass spectra are shown. For uncertainties affecting the shape, the range of values quoted represent the minimum and maximum effects over all bins. For the QCD multijets fit uncertainty of the resolved search, the values quoted are the combined effects of the shape and yield uncertainties of this background estimate. The symbols ^{*} and [†] denote uncertainties specific to the inclusive and *b*-tagged selections, respectively.

Search	Background	Source of systematic uncertainty	Effect	Value
Boosted	QCD multijets	Closure	Yield	10.0%
		Transfer factor fit	Shape	1.0%–4.0% [*] 3.0%–8.0% [†]
		Event count in region <i>C</i>	Shape	1.0%–23.0% [*] 2.0%–33.0% [†]
	Resonant	Simulation modeling	Yield	10.0%
		Statistical precision of simulation	Shape	1.0%–30.0% [*] 8.0%–57.0% [†]
			Shape and yield	3.0%–28.0% [*] 2.0%–38.0% [†]
Resolved	QCD multijets	Fit parameters	Shape and yield	3.0%–28.0% [*] 2.0%–38.0% [†]

have previously been observed [43]. We take these differences as estimates of the associated systematic errors.

Previous studies [43,44] have shown disagreement in the pruned jet mass spectra between data and simulation when a τ_{21} requirement is applied. The method used to quantify this discrepancy is described in Ref. [44], and is based on measuring the efficiency of identifying boosted two-prong *W* bosons in semileptonic $t\bar{t}$ events. For $\tau_{21} < 0.45$, the ratio of the efficiencies in data and simulation, or scale factor, is measured to be 1.10 ± 0.13 . Since this search requires two jets to satisfy the same τ_{21} selection, the square of the scale factor is applied to the signal events in simulation, resulting in a total two-prong scale factor of 1.21 ± 0.29 . A similar effect has been reported when applying the τ_{32} requirement [45]. In this case, a tag-and-probe procedure is used to measure the efficiency of identifying boosted three-prong hadronic top quarks in

semileptonic $t\bar{t}$ events. For $\tau_{32} < 0.54$, the ratio of the efficiencies in data and simulation is 1.07 ± 0.05 , and the efficiency for selecting misidentified boosted top quarks is 20%. However, in this search, we veto three-prong jets by requiring $\tau_{32} > 0.54$, which results in an anti-three-prong scale factor of 0.99 ± 0.01 for one jet, and 0.96 ± 0.02 when two jets satisfy this τ_{32} requirement. The uncertainties in the two-prong (τ_{21}) and the anti-three-prong (τ_{32}) scale factors are propagated as systematic uncertainty in the signal yield.

Finally, the uncertainties due to the limited numbers of simulated signal events also contribute to the systematic uncertainty affecting the shape of the \bar{m} distribution. A summary of the systematic uncertainties affecting the signal yield and shape are summarized in Table IV.

Figure 5 illustrates the average pruned jet mass spectrum for data and the background predictions for the inclusive

TABLE IV. Summary of the sources of systematic uncertainties for the signal samples. The values of the systematic uncertainties and whether they affect the overall event yield or the shape of the mass spectra are shown. For uncertainties affecting the shape, the range of values quoted represent the minimum and maximum effects over all bins. The symbols ^{*} and [†] denote uncertainties specific to the inclusive and *b*-tagged selections, respectively.

Search	Source of systematic uncertainty	Effect	Value
Boosted and resolved	Integrated luminosity	Yield	2.5%
		Yield	3.0%
	Pileup	Yield	1.0%
		Yield	1.0%
	Jet energy scale	Yield	1.2%–1.5%
		Shape	2.0%
	Jet energy resolution	Yield	1.8%–6.0%
		Shape	10.0%–14.0%
	Statistical precision of simulation	Shape	3.0%–37.0% [*] 6.0%–55.0% [†]
		Yield	1.0% [†]
Boosted	Two-prong scale factor	Yield	23.0%
	Anti-three-prong scale factor	Yield	2.0%

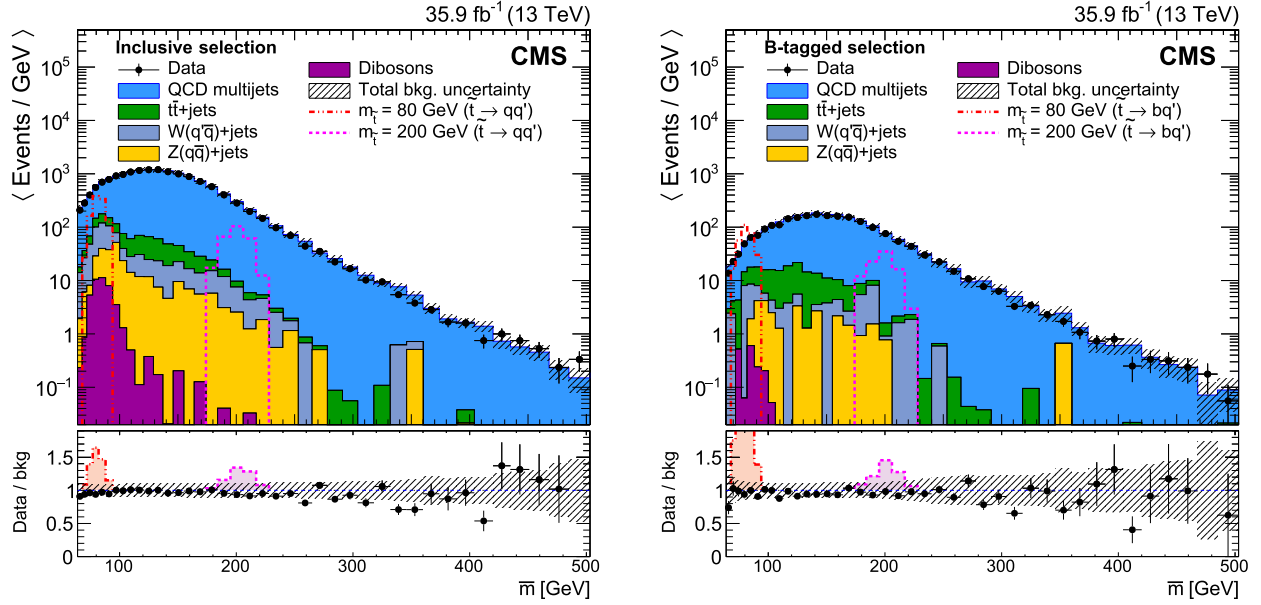


FIG. 5. Boosted search \bar{m} distribution for data (black points) and for the total background prediction, for the inclusive (left) and the b -tagged (right) selection. The different background components are presented with different colors, while the gray hashed band displays the total background uncertainty. The expected signals from simulated $\tilde{t} \rightarrow qq'$ and $\tilde{t} \rightarrow bq'$ samples at $m_{\tilde{t}} = 80$ GeV and $m_{\tilde{t}} = 200$ GeV are also displayed (shaded lines) for the inclusive selection and the b -tagged selections, respectively. The lower panel shows the ratio between data and the background prediction. The shaded peaks in the lower distributions show the expected effect produced by the presence of a top squark signal, for two different top squark masses.

(left) and the b -tagged (right) selections. The resonant backgrounds correspond to less than 8% of the total background prediction for the inclusive category, and less than 6% for the b -tagged one, over the entire mass range. The data are found to agree with SM expectations.

VI. RESOLVED SEARCH

A. Event selection

Events are selected using a logical OR of the H_T^{AK4} trigger, described in Sec. V, and two additional triggers: one requiring at least four AK4 jets with $p_T > 50$ GeV, $|\eta| < 2.5$, and $H_T^{\text{AK4}} > 800$ GeV, and another requiring at least four jets with $p_T > 70$ GeV, $|\eta| < 2.5$, and $H_T^{\text{AK4}} > 750$ GeV. In addition to satisfying the trigger conditions, selected events are required to have at least four AK4 jets with $p_T > 80$ GeV, $|\eta| < 2.5$, and $H_T^{\text{AK4}} > 900$ GeV. The selection efficiency of the chosen triggers is determined relative to unbiased data samples selected with muon based triggers. The trigger efficiency for events that would satisfy the subsequent selection is measured to be greater than 98%.

In order to select the two best dijet systems compatible with the signal, the four leading jets ordered in p_T are combined to create three unique combinations of dijet pairs per event. Out of the three combinations, the dijet configuration with the smallest ΔR_{dijet} is chosen. This variable is defined as $\Delta R_{\text{dijet}} = \sum_{i=1,2} |\Delta R^i - 0.8|$, where ΔR^i

represents the separation between two jets in the i th dijet pair, $\Delta R = \sqrt{(\Delta\eta)^2 + (\Delta\phi)^2}$, and $\Delta\eta$ and $\Delta\phi$ are the differences in η and azimuthal angle ϕ (in radians) between the two jets under consideration. This variable exploits the expectation that the decay products of the signal resonance will be closer together compared to particles from uncorrelated jets. An offset of 0.8 has been chosen in the definition of ΔR_{dijet} to avoid overlaps between jets in the dijet systems, and to minimize the selection of dijet systems composed of jets from radiated gluons.

Once a configuration is selected, the average mass of the dijet system, $\bar{M} = (m_{\text{jj1}} + m_{\text{jj2}})/2$, is used to search for new resonances, where $m_{\text{jj}i}$ is the dijet mass of the i th dijet. To further reject backgrounds from QCD multijet events and incorrect pairings from signal events, two additional requirements are applied. As was described in Sec. V, the dijet systems in signal events are expected to be more centrally produced than those in QCD multijet events; therefore, the pseudorapidity difference between the two dijet systems is required to be $\Delta\eta_{\text{dijet}} = |\eta_{\text{jj1}} - \eta_{\text{jj2}}| < 1.0$. In addition, further discrimination is achieved by requiring the mass asymmetry (M_{asym}) between the dijet pairs to be < 0.1 , where $M_{\text{asym}} = |m_{\text{jj1}} - m_{\text{jj2}}| / (m_{\text{jj1}} + m_{\text{jj2}})$. Figures 6 and 7 show the discriminating power of these two kinematic variables applied to data, QCD multijet simulation, and a selected simulated signal sample.

An additional variable defined as $\Delta = (\sum_{i=1,2} |p_T^i|) - \bar{M}$ is calculated for each dijet system, where the p_T sum is over

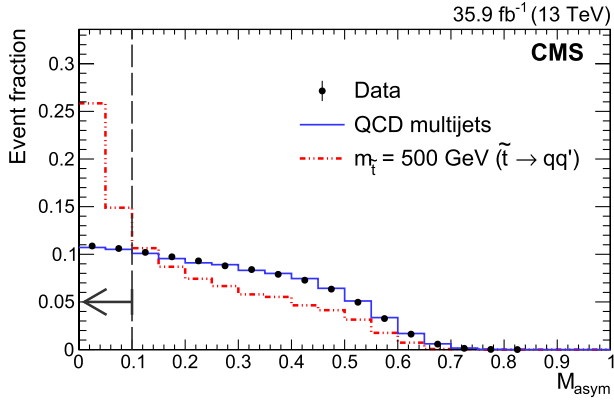


FIG. 6. Resolved search M_{asym} distribution normalized to unity for data (black dots), background (solid blue line), and a selected signal $\tilde{t} \rightarrow qq'$ with $m_{\tilde{t}} = 500$ GeV (dashed red line). All inclusive selection criteria are applied apart from that on the variable being presented. The region to the left of the black dashed line indicates the optimized region of selected M_{asym} values.

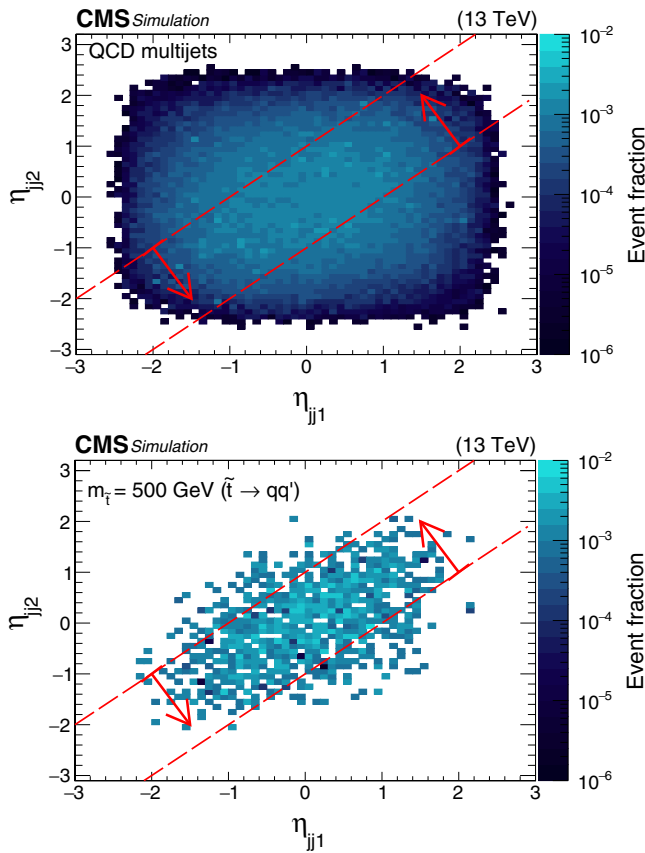


FIG. 7. Resolved search distribution of η_{jj2} of the lower- p_T dijet system in the selected pair as a function of the η_{jj1} of the higher- p_T dijet system. The distribution is shown for simulated QCD multijet events (left) and a representative signal $\tilde{t} \rightarrow qq'$ with $m_{\tilde{t}} = 500$ GeV (right). All inclusive selection criteria are applied apart from that on the variable being presented. The region between the two red dashed lines indicates the optimized region of selected $\Delta\eta_{\text{dijet}}$ values.

the two jets in the dijet configuration. The distributions of the Δ variable as a function of \bar{M} for a selected signal sample and QCD multijet simulation are illustrated in Fig. 8. This variable has been previously used in hadronic resonance searches at both the Tevatron and the LHC [8,46–50]. In addition to rejecting background events, setting a minimum value of Δ results in a lowering of the peak position of the \bar{M} distribution in SM QCD multijet events, and allows the search to be extended to lower resonance masses. Events are selected with $\Delta > 200$ GeV. Finally, for the b -tagged selection, a loose b -tagged jet is required in each dijet pair candidate. The selection requirements for this search are summarized in Table I (third column), and are found to be optimal for the entire range of masses considered here.

B. Background estimate

Events originating from QCD multijet processes dominate the \bar{M} spectrum and are modeled with the following function:

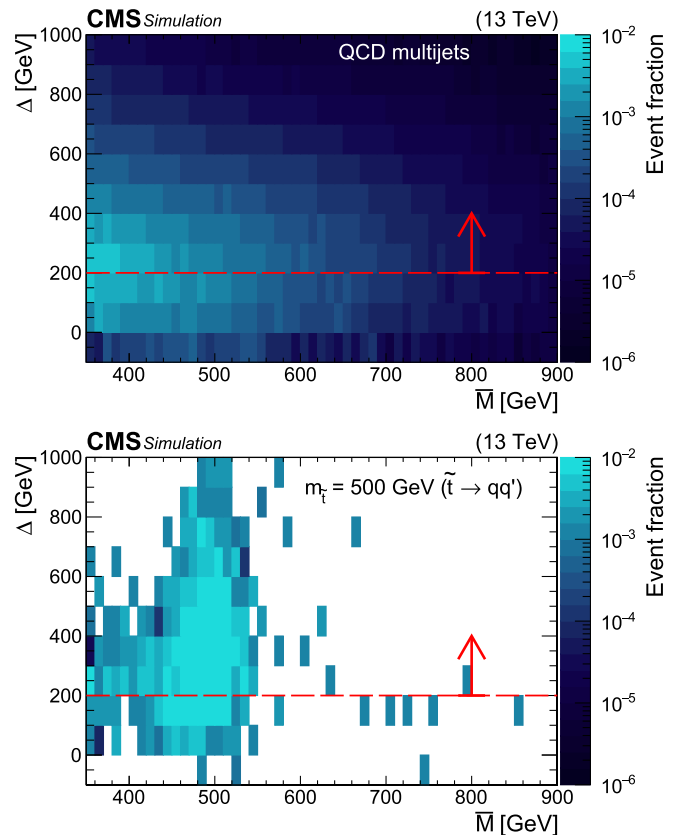


FIG. 8. Resolved search distribution of Δ as a function of \bar{M} , shown for simulated QCD multijet events (left) and a representative signal $\tilde{t} \rightarrow qq'$ with $m_{\tilde{t}} = 500$ GeV (right). All inclusive selection criteria are applied apart from that on the variable being presented. The region above the red dashed line indicates the optimized region of selected Δ values.

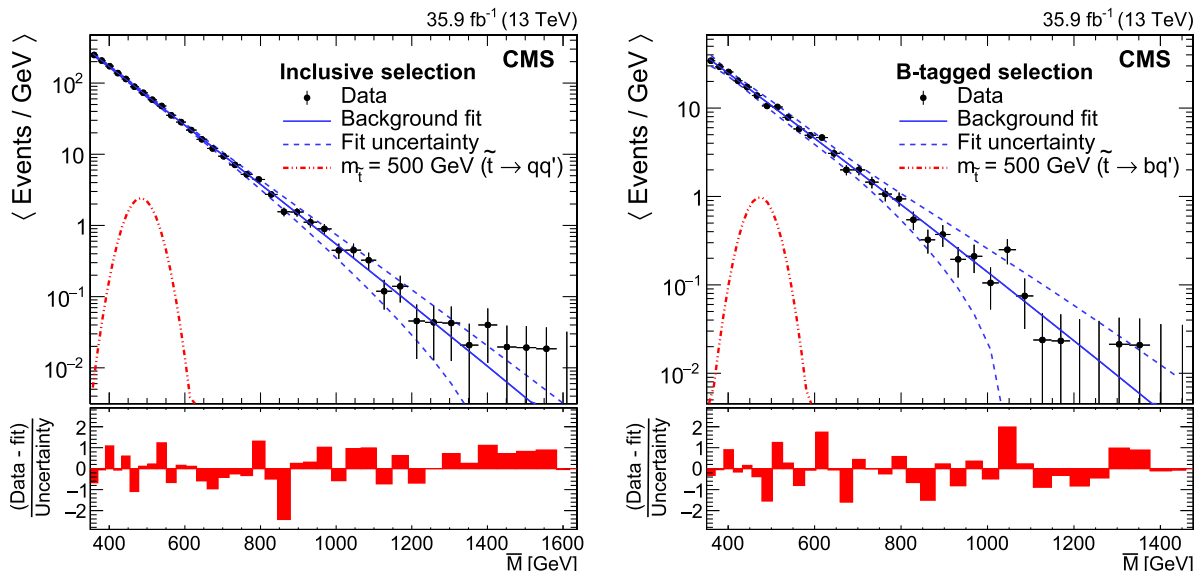


FIG. 9. Resolved search distribution of \bar{M} for the data (black points), along with the resulting fit to the functional form in Eq. (3) (blue solid line) for the inclusive selection (left) and the b -tagged (right) selections. The expected signals from simulated $\tilde{t} \rightarrow qq'$ and $\tilde{t} \rightarrow bq'$ samples at $m_{\tilde{t}} = 500$ GeV are also displayed (red dot-dashed lines) for the inclusive selection and the b -tagged selections, respectively. The lower panel displays the bin-by-bin difference between the data and the fit divided by the statistical uncertainty.

$$\frac{dN}{d\bar{M}} = \frac{p_0(1-x)^{p_1}}{x^{p_2}}, \quad (3)$$

where $x = \bar{M}/\sqrt{s}$, \sqrt{s} is the center-of-mass energy, N is the number of considered events, and p_0 through p_2 are parameters of the function. The functional form in Eq. (3) successfully models the steeply falling dijet mass distribution of QCD multijet production, and comparable functions have been extensively used in similar previous dijet resonance searches [8,43,51].

Figure 9 illustrates the fitted \bar{M} distributions in data using the inclusive (left) and the b -tagged (right) selections for the resolved analysis. The parametrized fit is performed for $\bar{M} > 350$ GeV for both selections. In this region the background is well modeled by the parametrization and the trigger has an efficiency greater than 98% as a function of \bar{M} . Figure 9 (lower panels) shows the bin-by-bin difference between the data and the fit divided by the statistical uncertainty. The data agree with SM expectations.

The potential bias introduced by the choice of the background parametrization was investigated by performing signal injection tests in pseudoexperiments. The pseudoexperiments were generated using the mass spectra from simulated signal events fitted with a Gaussian function, added to that of the QCD multijet simulation fitted with the function of Eq. (3). Each pseudoexperiment was then fitted with alternative parametrizations from different families of functions of varying orders, and the effect on the strength of the injected signal was estimated and found to be negligible.

C. Signal efficiency and systematic uncertainties

The \bar{M} distributions of the simulated signal samples are parametrized with Gaussian functions, and are shown for the inclusive selection in Fig. 10 (left). Similar signal mass shapes are found in the b -tagged analysis. The signal efficiency for the resolved search is illustrated in Fig. 10 (right) for both the inclusive and the b -tagged selections. The fraction of $\tilde{t} \rightarrow qq'$ signal events remaining in simulation after applying the inclusive selection, relative to the total number of events generated, is between 0.66 and 1.16% for $m_{\tilde{t}}$ between 400 and 1500 GeV. In the b -tagged selection, the fraction of remaining events in the $\tilde{t} \rightarrow bq'$ simulation is between 0.12 and 0.42% for $m_{\tilde{t}}$ between 400 and 1400 GeV.

The sources of systematic uncertainties affecting the normalization of the expected signal contribution are the integrated luminosity measurement (2.5%) [12], the trigger efficiency (3.0%), the modeling of the pileup interactions (1.0%), and the choice of PDF set (1.0%) [42]. The uncertainties in the measurement of the jet energy scale (1.5%) and resolution (6.0%) [32,33] introduce both a change in the yield and the shape of the \bar{M} spectrum. For the b -tagged selection, the uncertainty in the efficiency for identifying bottom quarks (1.0%) contributes to the overall uncertainty in the expected signal yield [39]. Finally, the statistical uncertainties associated with the simulated samples also contribute to the overall systematic uncertainty. The systematic uncertainties affecting the signal are summarized in Table IV.

The uncertainties in the fitted parameters of Eq. (3) are also taken into account as sources of systematic uncertainty

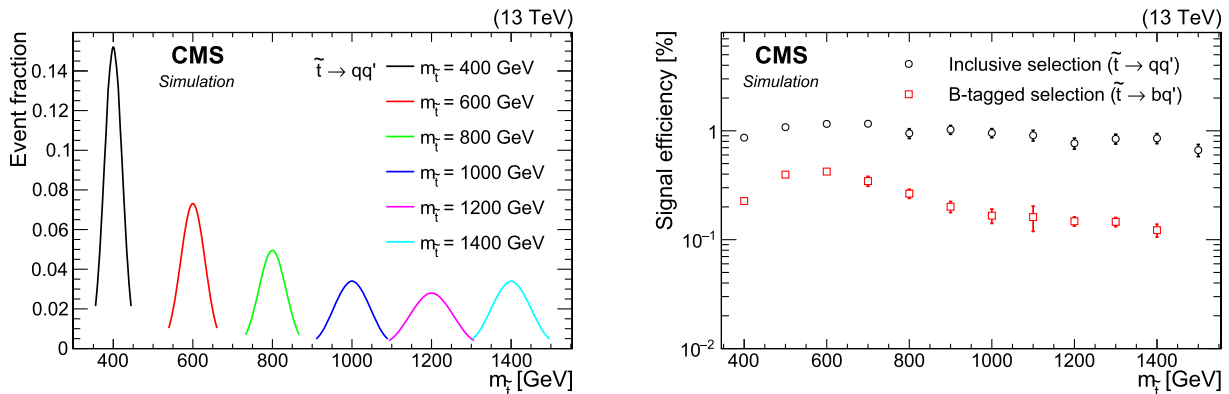


FIG. 10. Simulated signal distributions for the resolved search. Left: Gaussian fits to the mass of the simulated signals for various $m_{\tilde{t}}$ probed in this search for the inclusive selection. Right: signal efficiency, as a function of $m_{\tilde{t}}$, for the inclusive and b -tagged selections.

affecting both the background yield and shape of the \overline{M} spectrum, and are summarized in Table III.

VII. RESULTS

Figures 5 and 9 present the mass spectra for the boosted and resolved analyses, respectively. They are in agreement with SM expectations. The mass spectra are used to set limits on the pair production cross section as a function of mass of resonances decaying into quark pairs, by considering the benchmark model of top squarks decaying via the RPV couplings λ''_{312} and λ''_{323} . The exclusion limits are computed using the modified frequentist approach for C.L., with a binned profile likelihood as the test statistic [52,53], using an asymptotic approximation [54].

Results for the boosted search are obtained from combined signal and background binned likelihood fits to the \overline{m} distribution in data. For each value of $m_{\tilde{t}}$ considered, only bins of \overline{m} within two standard deviations of the mean of a

Gaussian function fitted to the generated top squark mass are included in the likelihood. For each bin used in the likelihood, the individual background components and the signal are allowed to float within uncertainties. Systematic uncertainties affecting the yield and the shape, as summarized in Tables III and IV, are assumed to be correlated among bins. These uncertainties are treated as nuisance parameters, which are profiled and modeled with log-normal priors, except for the uncertainty in the number of events in sideband region C, which is modeled with a Γ function prior.

For the resolved search, the \overline{M} spectrum in data is compared to the background fit to search for localized deviations consistent with a resonance. For each value of $m_{\tilde{t}}$, a likelihood fit is used to compare the data to the shapes for the signal and background, within a mass window of two standard deviations around the true value of $m_{\tilde{t}}$. Here, all systematic uncertainties are modeled with log-normal priors.

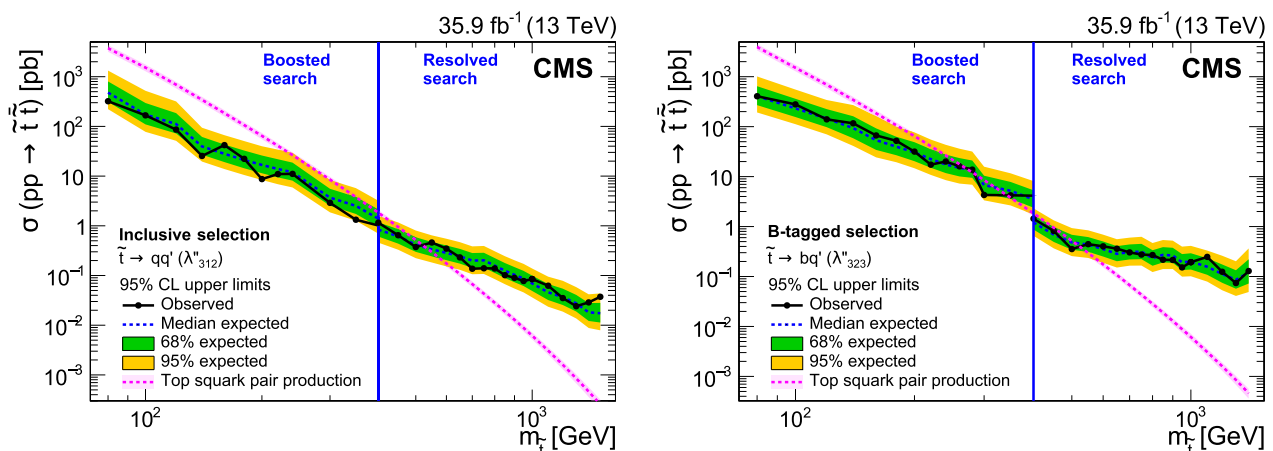


FIG. 11. Observed and expected 95% CL upper limits on the signal cross section as a function of $m_{\tilde{t}}$. The branching fraction to quarks is assumed to be 100%. The boosted analysis probes $80 \leq m_{\tilde{t}} < 400$ GeV, while the resolved analysis searches for $m_{\tilde{t}} \geq 400$ GeV. Left: limits using the inclusive selection for $\tilde{t} \rightarrow qq'$ assuming the RPV coupling λ''_{312} . Right: limits using the b -tagged selection for $\tilde{t} \rightarrow bq'$ assuming the RPV coupling λ''_{323} . The dashed pink line shows the NLO + NLL theoretical prediction for top squark pair production [40,41].

Figure 11 shows the observed and expected 95% CL upper limits on the top squark pair production of cross section as a function of $m_{\tilde{t}}$ for the boosted and resolved analyses. The boosted analysis probes the mass range $80 \leq m_{\tilde{t}} < 400$ GeV, while the resolved analysis covers the range $m_{\tilde{t}} \geq 400$ GeV. Figure 11 (left) presents the resulting limits using the inclusive selection for the λ''_{312} coupling scenario, while Fig. 11 (right) illustrates the limits using the b -tagged selection assuming the λ''_{323} coupling. The dashed pink line represents the theoretical prediction for the top squark pair production cross section at $\sqrt{s} = 13$ TeV evaluated at NLO with next-to-leading logarithmic (NLL) corrections [40,41]. We exclude top squark masses from 80 to 520 GeV assuming the λ''_{312} coupling. For the λ''_{323} coupling, the boosted search excludes masses from 80 to 270 and from 285 to 340 GeV; and the resolved search excludes masses from 400 to 525 GeV. The corresponding expected mass limits obtained are 80 to 520 GeV for top squarks decaying via λ''_{312} , and 80 to 270, 285 to 320, and 400 to 505 GeV for the λ''_{323} coupling.

VIII. SUMMARY

A search has been performed for the pair production of diquark resonances in two-jet events in a boosted jet topology and in four-jet events in a resolved jet topology. Data from proton-proton collisions at $\sqrt{s} = 13$ TeV collected in 2016 with the CMS detector, corresponding to an integrated luminosity of 35.9 fb^{-1} , have been analysed. In the boosted search, the distribution of the average mass of the selected two jets has been investigated for localized disagreements between data and the background estimate, consistent with the presence of a narrow resonance, while in the resolved analysis the average mass of the selected dijet pairs is utilized. The boosted search explores resonance masses between 80 and 400 GeV, while the resolved one covers masses above 400 GeV. We find agreement between the observation and standard model expectations. These results are interpreted in the framework of R -parity-violating supersymmetry with the pair production of top squarks decaying promptly to quarks via the λ''_{312} or the λ''_{323} couplings, assuming 100% branching fractions to $\tilde{t} \rightarrow qq'$ or $\tilde{t} \rightarrow bq'$, respectively. Upper limits are set at 95% confidence level on the pair production cross section of top squarks as a function of the top squark mass. We exclude top squark masses with the λ''_{312} coupling from 80 to 520 GeV. For the λ''_{323} coupling, the boosted search excludes masses from 80 to 270 and from 285 to 340 GeV; and the resolved search excludes masses from 400 to 525 GeV. These results probe a wider range of masses than previously explored at the LHC, and extend the top squark mass limits in the $\tilde{t} \rightarrow qq'$ scenario.

ACKNOWLEDGMENTS

We congratulate our colleagues in the CERN accelerator departments for the excellent performance of the LHC and

thank the technical and administrative staffs at CERN and at other CMS institutes for their contributions to the success of the CMS effort. In addition, we gratefully acknowledge the computing centers and personnel of the Worldwide LHC Computing Grid for delivering so effectively the computing infrastructure essential to our analyses. Finally, we acknowledge the enduring support for the construction and operation of the LHC and the CMS detector provided by the following funding agencies: BMBWF and FWF (Austria); FNRS and FWO (Belgium); CNPq, CAPES, FAPERJ, FAPERGS, and FAPESP (Brazil); MES (Bulgaria); CERN; CAS, MoST, and NSFC (China); COLCIENCIAS (Colombia); MSES and CSF (Croatia); RPF (Cyprus); SENESCYT (Ecuador); MoER, ERC IUT, and ERDF (Estonia); Academy of Finland, MEC, and HIP (Finland); CEA and CNRS/IN2P3 (France); BMBF, DFG, and HGF (Germany); GSRT (Greece); NKfIA (Hungary); DAE and DST (India); IPM (Iran); SFI (Ireland); INFN (Italy); MSIP and NRF (Republic of Korea); MES (Latvia); LAS (Lithuania); MOE and UM (Malaysia); BUAP, CINVESTAV, CONACYT, LNS, SEP, and UASLP-FAI (Mexico); MOS (Montenegro); MBIE (New Zealand); PAEC (Pakistan); MSHE and NSC (Poland); FCT (Portugal); JINR (Dubna); MON, RosAtom, RAS, RFBR, and NRC KI (Russia); MESTD (Serbia); SEIDI, CPAN, PCTI, and FEDER (Spain); MOSTR (Sri Lanka); Swiss Funding Agencies (Switzerland); MST (Taipei); ThEPCenter, IPST, STAR, and NSTDA (Thailand); TUBITAK and TAEK (Turkey); NASU and SFFR (Ukraine); STFC (United Kingdom); DOE and NSF (USA). Individuals have received support from the Marie-Curie program and the European Research Council and Horizon 2020 Grant, Contract No. 675440 (European Union); the Leventis Foundation; the A. P. Sloan Foundation; the Alexander von Humboldt Foundation; the Belgian Federal Science Policy Office; the Fonds pour la Formation à la Recherche dans l'Industrie et dans l'Agriculture (FRRIA-Belgium); the Agentschap voor Innovatie door Wetenschap en Technologie (IWT-Belgium); the F. R. S.-FNRS and FWO (Belgium) under the “Excellence of Science—EOS”—be.h Project No. 30820817; the Ministry of Education, Youth and Sports (MEYS) of the Czech Republic; the Lendület (“Momentum”) Program and the János Bolyai Research Scholarship of the Hungarian Academy of Sciences, the New National Excellence Program ÚNKP, the NKfIA research Grants No. 123842, No. 123959, No. 124845, No. 124850, and No. 125105 (Hungary); the Council of Science and Industrial Research, India; the HOMING PLUS program of the Foundation for Polish Science, cofinanced from European Union, Regional Development Fund, the Mobility Plus program of the Ministry of Science and Higher Education, the National Science Center (Poland), Contracts No. Harmonia 2014/14/M/ST2/00428, No. Opus 2014/13/B/ST2/02543,

No. 2014/15/B/ST2/03998, and No. 2015/19/B/ST2/02861, No. Sonata-bis 2012/07/E/ST2/01406; the National Priorities Research Program by Qatar National Research Fund; the Programa Estatal de Fomento de la Investigación Científica y Técnica de Excelencia María de Maeztu, Grant No. MDM-2015-0509 and the Programa Severo Ochoa del Principado de Asturias; the Thalís and

Aristeia programs cofinanced by EU-ESF and the Greek NSRF; the Rachadapisek Sompot Fund for Postdoctoral Fellowship, Chulalongkorn University and the Chulalongkorn Academic into Its 2nd Century Project Advancement Project (Thailand); the Welch Foundation, Contract No. C-1845; and the Weston Havens Foundation (USA).

-
- [1] C. Kilic, T. Okui, and R. Sundrum, Colored resonances at the Tevatron: Phenomenology and discovery potential in multijets, *J. High Energy Phys.* **07** (2008) 038.
- [2] C. T. Hill, Topcolor: Top quark condensation in a gauge extension of the standard model, *Phys. Lett. B* **266**, 419 (1991).
- [3] G. D. Kribs, E. Poppitz, and N. Weiner, Flavor in supersymmetry with an extended R-symmetry, *Phys. Rev. D* **78**, 055010 (2008).
- [4] J. A. Evans and Y. Kats, LHC coverage of RPV MSSM with light stops, *J. High Energy Phys.* **04** (2013) 028.
- [5] R. Barbier, C. Berat, M. Besancon, M. Chemtob, A. Deandrea, E. Dudas, P. Fayet, S. Lavignac, G. Moreau, E. Perez, and Y. Sirois, R-parity violating supersymmetry, *Phys. Rep.* **420**, 1 (2005).
- [6] A. Heister *et al.* (ALEPH Collaboration), Search for supersymmetric particles with R parity violating decays in e^+e^- collisions at \sqrt{s} up to 209 GeV, *Eur. Phys. J. C* **31**, 1 (2003).
- [7] T. Aaltonen *et al.* (CDF Collaboration), Search for Pair Production of Strongly Interacting Particles Decaying to Pairs of Jets in $p\bar{p}$ Collisions at $\sqrt{s} = 1.96$ TeV, *Phys. Rev. Lett.* **111**, 031802 (2013).
- [8] CMS Collaboration, Search for pair-produced resonances decaying to jet pairs in proton-proton collisions at $\sqrt{s} = 8$ TeV, *Phys. Lett. B* **747**, 98 (2015).
- [9] ATLAS Collaboration, A search for pair-produced resonances in four-jet final states at $\sqrt{s} = 13$ TeV with the ATLAS detector, *Eur. Phys. J. C* **78**, 250 (2018).
- [10] ATLAS Collaboration, A search for top squarks with R-parity-violating decays to all-hadronic final states with the ATLAS detector in $\sqrt{s} = 8$ TeV proton-proton collisions, *J. High Energy Phys.* **06** (2016) 067.
- [11] CMS Collaboration, The CMS experiment at the CERN LHC, *J. Instrum.* **3**, S08004 (2008).
- [12] CMS Collaboration, CMS luminosity measurements for the 2016 data taking period, CMS Physics Analysis Summary, CERN Report No. CMS-PAS-LUM-17-001, 2017, <https://cds.cern.ch/record/2257069>.
- [13] CMS Collaboration, The CMS trigger system, *J. Instrum.* **12**, P01020 (2017).
- [14] T. Sjöstrand, S. Ask, J. R. Christiansen, R. Corke, N. Desai, P. Ilten, S. Mrenna, S. Prestel, C. O. Rasmussen, and P. Z. Skands, An introduction to PYTHIA 8.2, *Comput. Phys. Commun.* **191**, 159 (2015).
- [15] J. Alwall, R. Frederix, S. Frixione, V. Hirschi, F. Maltoni, O. Mattelaer, H. S. Shao, T. Stelzer, P. Torrielli, and M. Zaro, The automated computation of tree-level and next-to-leading order differential cross sections, and their matching to parton shower simulations, *J. High Energy Phys.* **07** (2014) 079.
- [16] J. Alwall, S. Höche, F. Krauss, N. Lavesson, L. Lönnblad, F. Maltoni, M. L. Mangano, M. Moretti, C. G. Papadopoulos, F. Piccinini, S. Schumann, M. Treccani, J. Winter, and M. Worek, Comparative study of various algorithms for the merging of parton showers and matrix elements in hadronic collisions, *Eur. Phys. J. C* **53**, 473 (2008).
- [17] CMS Collaboration, Event generator tunes obtained from underlying event and multiparton scattering measurements, *Eur. Phys. J. C* **76**, 155 (2016).
- [18] R. Frederix and S. Frixione, Merging meets matching in MC@NLO, *J. High Energy Phys.* **12** (2012) 061.
- [19] S. Alioli, S.-O. Moch, and P. Uwer, Hadronic top-quark pair-production with one jet and parton showering, *J. High Energy Phys.* **01** (2012) 137.
- [20] T. Melia, P. Nason, R. Rontsch, and G. Zanderighi, W^+W^+ plus dijet production in the POWHEGBOX, *Eur. Phys. J. C* **71**, 1670 (2011).
- [21] S. Kallweit, J. M. Lindert, P. Maierhofer, S. Pozzorini, and M. Schönherr, NLO QCD + EW predictions for V + jets including off-shell vector-boson decays and multijet merging, *J. High Energy Phys.* **04** (2016) 021.
- [22] S. Kallweit, J. M. Lindert, S. Pozzorini, M. Schönherr, and P. Maierhofer, NLO QCD + EW automation and precise predictions for V + multijet production, in *Proceedings of the 50th Rencontres de Moriond, QCD and high energy interactions: La Thuile, Italy, 2015* (2015), p. 121, <https://inspirehep.net/record/1372103>.
- [23] J. M. Lindert *et al.*, Precise predictions for V + jets dark matter backgrounds, *Eur. Phys. J. C* **77**, 829 (2017).
- [24] CMS Collaboration, Search for dark matter produced with an energetic jet or a hadronically decaying W or Z boson at $\sqrt{s} = 13$ TeV, *J. High Energy Phys.* **07** (2017) 014.
- [25] S. Kallweit, J. M. Lindert, P. Maierhofer, S. Pozzorini, and M. Schönherr, NLO electroweak automation and precise predictions for W + multijet production at the LHC, *J. High Energy Phys.* **04** (2015) 012.
- [26] S. Agostinelli *et al.* (GEANT4 Collaboration), GEANT4—A simulation toolkit, *Nucl. Instrum. Methods Phys. Res., Sect. A* **506**, 250 (2003).
- [27] R. D. Ball *et al.* (NNPDF Collaboration), Parton distributions for the LHC Run II, *J. High Energy Phys.* **04** (2015) 040.

- [28] M. Cacciari, G. P. Salam, and G. Soyez, The anti- k_T jet clustering algorithm, *J. High Energy Phys.* **04** (2008) 063.
- [29] M. Cacciari, G. P. Salam, and G. Soyez, FastJet user manual, *Eur. Phys. J. C* **72**, 1896 (2012).
- [30] CMS Collaboration, Particle-flow reconstruction and global event description with the CMS detector, *J. Instrum.* **12**, P10003 (2017).
- [31] M. Cacciari and G. P. Salam, Pileup subtraction using jet areas, *Phys. Lett. B* **659**, 119 (2008).
- [32] CMS Collaboration, Jet energy scale and resolution in the CMS experiment in pp collisions at 8 TeV, *J. Instrum.* **12**, P02014 (2017).
- [33] CMS Collaboration, Determination of jet energy calibration and transverse momentum resolution in CMS, *J. Instrum.* **6**, P11002 (2011).
- [34] D. Krohn, J. Thaler, and L.-T. Wang, Jet trimming, *J. High Energy Phys.* **02** (2010) 084.
- [35] S. D. Ellis, C. K. Vermilion, and J. R. Walsh, Recombination algorithms and jet substructure: Pruning as a tool for heavy particle searches, *Phys. Rev. D* **81**, 094023 (2010).
- [36] S. Catani, Y. L. Dokshitzer, M. H. Seymour, and B. R. Webber, Longitudinally invariant K_T clustering algorithms for hadron hadron collisions, *Nucl. Phys.* **B406**, 187 (1993).
- [37] M. Wobisch and T. Wengler, Hadronization corrections to jet cross-sections in deep inelastic scattering, in Monte Carlo Generators for HERA Physics. Proceedings of the Workshop, Hamburg, Germany (DESY, Hamburg, Germany, 1998), p. 270, <https://inspirehep.net/record/484872>.
- [38] J. Thaler and K. Van Tilburg, Maximizing boosted top identification by minimizing N -subjettiness, *J. High Energy Phys.* **02** (2012) 093.
- [39] CMS Collaboration, Identification of heavy-flavour jets with the CMS detector in pp collisions at 13 TeV, *J. Instrum.* **13**, P05011 (2018).
- [40] C. Borschensky, M. Krämer, A. Kulesza, M. Mangano, S. Padhi, T. Plehn, and X. Portell, Squark and gluino production cross sections in pp collisions at $\sqrt{s} = 13, 14, 33$ and 100 TeV, *Eur. Phys. J. C* **74**, 3174 (2014).
- [41] W. Beenakker, C. Borschensky, M. Krämer, A. Kulesza, E. Laenen, S. Marzani, and J. Rojo, NLO + NLL squark and gluino production cross-sections with threshold-improved parton distributions, *Eur. Phys. J. C* **76**, 53 (2016).
- [42] J. Rojo, PDF4LHC recommendations for Run II, Proc. Sci. DIS2016 (2016) 018 [arXiv:1606.08243].
- [43] CMS Collaboration, Search for massive resonances decaying into WW , WZ , ZZ , qW , and qZ with dijet final states at $\sqrt{s} = 13$ TeV, *Phys. Rev. D* **97**, 072006 (2018).
- [44] CMS Collaboration, Identification techniques for highly boosted W bosons that decay into hadrons, *J. High Energy Phys.* **12** (2014) 017.
- [45] CMS Collaboration, Jet algorithms performance in 13 TeV data, CMS Physics Analysis Summary Report No. CMS-PAS-JME-16-003, 2017, <https://cds.cern.ch/record/2256875>.
- [46] T. Aaltonen *et al.* (CDF Collaboration), First Search for Multijet Resonances in $\sqrt{s} = 1.96$ TeV $p\bar{p}$ Collisions, *Phys. Rev. Lett.* **107**, 042001 (2011).
- [47] CMS Collaboration, Search for Three-Jet Resonances in pp Collisions at $\sqrt{s} = 7$ TeV, *Phys. Rev. Lett.* **107**, 101801 (2011).
- [48] CMS Collaboration, Search for three-jet resonances in pp collisions at $\sqrt{s} = 7$ TeV, *Phys. Lett. B* **718**, 329 (2012).
- [49] CMS Collaboration, Searches for light- and heavy-flavour three-jet resonances in pp collisions at $\sqrt{s} = 8$ TeV, *Phys. Lett. B* **730**, 193 (2014).
- [50] CMS Collaboration, Search for Pair-Produced Dijet Resonances in Four-Jet Final States in Proton-Proton Collisions at $\sqrt{s} = 7$ TeV, *Phys. Rev. Lett.* **110**, 141802 (2013).
- [51] CMS Collaboration, Search for Narrow Resonances Decaying to Dijets in Proton-Proton Collisions at $\sqrt{s} = 13$ TeV, *Phys. Rev. Lett.* **116**, 071801 (2016).
- [52] T. Junk, Confidence level computation for combining searches with small statistics, *Nucl. Instrum. Methods Phys. Res., Sect. A* **434**, 435 (1999).
- [53] A. L. Read, Presentation of search results: The CL_s technique, *J. Phys. G* **28**, 2693 (2002).
- [54] G. Cowan, K. Cranmer, E. Gross, and O. Vitells, Erratum: Asymptotic formulae for likelihood-based tests of new physics, *Eur. Phys. J. C* **71**, 1554 (2011).

A. M. Sirunyan,¹ A. Tumasyan,¹ W. Adam,² F. Ambrogio,² E. Asilar,² T. Bergauer,² J. Brandstetter,² M. Dragicevic,² J. Erö,² A. Escalante Del Valle,² M. Flechl,² R. Frühwirth,^{2,b} V. M. Ghete,² J. Hrubec,² M. Jeitler,^{2,b} N. Krammer,² I. Krätschmer,² D. Liko,² T. Madlener,² I. Mikulec,² N. Rad,² H. Rohringer,² J. Schieck,^{2,b} R. Schöfbeck,² M. Spanring,² D. Spitzbart,² A. Taurok,² W. Waltenberger,² J. Wittmann,² C.-E. Wulz,^{2,b} M. Zarucki,² V. Chekhovsky,³ V. Mossolov,³ J. Suarez Gonzalez,³ E. A. De Wolf,⁴ D. Di Croce,⁴ X. Janssen,⁴ J. Lauwers,⁴ M. Pieters,⁴ H. Van Haevermaet,⁴ P. Van Mechelen,⁴ N. Van Remortel,⁴ S. Abu Zeid,⁵ F. Blekman,⁵ J. D'Hondt,⁵ I. De Bruyn,⁵ J. De Clercq,⁵ K. Deroover,⁵ G. Flouris,⁵ D. Lontkovskiy,⁵ S. Lowette,⁵ I. Marchesini,⁵ S. Moortgat,⁵ L. Moreels,⁵ Q. Python,⁵ K. Skovpen,⁵ S. Tavernier,⁵ W. Van Doninck,⁵ P. Van Mulders,⁵ I. Van Parijs,⁵ D. Beghin,⁶ B. Bilin,⁶ H. Brun,⁶ B. Clerbaux,⁶ G. De Lentdecker,⁶ H. Delannoy,⁶ B. Dorney,⁶ G. Fasanella,⁶ L. Favart,⁶ R. Goldouzian,⁶ A. Grebenyuk,⁶ A. K. Kalsi,⁶ T. Lenzi,⁶ J. Luetic,⁶ N. Postiau,⁶ E. Starling,⁶ L. Thomas,⁶ C. Vander Velde,⁶ P. Vanlaer,⁶ D. Vannerom,⁶ Q. Wang,⁶ T. Cornelis,⁷ D. Dobur,⁷ A. Fagot,⁷ M. Gul,⁷ I. Khvastunov,^{7,c} D. Poyraz,⁷ C. Roskas,⁷ D. Trocino,⁷ M. Tytgat,⁷ W. Verbeke,⁷ B. Vermassen,⁷ M. Vit,⁷ N. Zaganidis,⁷ H. Bakhshiansohi,⁸ O. Bondu,⁸ S. Brochet,⁸ G. Bruno,⁸ C. Caputo,⁸ P. David,⁸ C. Delaere,⁸ M. Delcourt,⁸ B. Francois,⁸ A. Giammanco,⁸ G. Krintiras,⁸ V. Lemaître,⁸ A. Magitter,⁸ A. Mertens,⁸

M. Musich,⁸ K. Piotrkowski,⁸ A. Saggio,⁸ M. Vidal Marono,⁸ S. Wertz,⁸ J. Zobec,⁸ F. L. Alves,⁹ G. A. Alves,⁹ M. Correa Martins Junior,⁹ G. Correia Silva,⁹ C. Hensel,⁹ A. Moraes,⁹ M. E. Pol,⁹ P. Rebello Teles,⁹ E. Belchior Batista Das Chagas,¹⁰ W. Carvalho,¹⁰ J. Chinellato,^{10,d} E. Coelho,¹⁰ E. M. Da Costa,¹⁰ G. G. Da Silveira,^{10,e} D. De Jesus Damiao,¹⁰ C. De Oliveira Martins,¹⁰ S. Fonseca De Souza,¹⁰ H. Malbouisson,¹⁰ D. Matos Figueiredo,¹⁰ M. Melo De Almeida,¹⁰ C. Mora Herrera,¹⁰ L. Mundim,¹⁰ H. Nogima,¹⁰ W. L. Prado Da Silva,¹⁰ L. J. Sanchez Rosas,¹⁰ A. Santoro,¹⁰ A. Sznajder,¹⁰ M. Thiel,¹⁰ E. J. Tonelli Manganote,^{10,d} F. Torres Da Silva De Araujo,¹⁰ A. Vilela Pereira,¹⁰ S. Ahuja,^{11a} C. A. Bernardes,^{11a} L. Calligaris,^{11a} T. R. Fernandez Perez Tomei,^{11a} E. M. Gregores,^{11a,11b} P. G. Mercadante,^{11a,11b} S. F. Novaes,^{11a} Sandra S. Padula,^{11a} A. Aleksandrov,¹² R. Hadjiiska,¹² P. Iaydjiev,¹² A. Marinov,¹² M. Misheva,¹² M. Rodozov,¹² M. Shopova,¹² G. Sultanov,¹² A. Dimitrov,¹³ L. Litov,¹³ B. Pavlov,¹³ P. Petkov,¹³ W. Fang,^{14,f} X. Gao,^{14,f} L. Yuan,¹⁴ M. Ahmad,¹⁵ J. G. Bian,¹⁵ G. M. Chen,¹⁵ H. S. Chen,¹⁵ M. Chen,¹⁵ Y. Chen,¹⁵ C. H. Jiang,¹⁵ D. Leggat,¹⁵ H. Liao,¹⁵ Z. Liu,¹⁵ F. Romeo,¹⁵ S. M. Shaheen,^{15,g} A. Spiezia,¹⁵ J. Tao,¹⁵ Z. Wang,¹⁵ E. Yazgan,¹⁵ H. Zhang,¹⁵ S. Zhang,^{15,g} J. Zhao,¹⁵ Y. Ban,¹⁶ G. Chen,¹⁶ A. Levin,¹⁶ J. Li,¹⁶ L. Li,¹⁶ Q. Li,¹⁶ Y. Mao,¹⁶ S. J. Qian,¹⁶ D. Wang,¹⁶ Z. Xu,¹⁶ Y. Wang,¹⁷ C. Avila,¹⁸ A. Cabrera,¹⁸ C. A. Carrillo Montoya,¹⁸ L. F. Chaparro Sierra,¹⁸ C. Florez,¹⁸ C. F. González Hernández,¹⁸ M. A. Segura Delgado,¹⁸ B. Courbon,¹⁹ N. Godinovic,¹⁹ D. Lelas,¹⁹ I. Puljak,¹⁹ T. Sculac,¹⁹ Z. Antunovic,²⁰ M. Kovac,²⁰ V. Brigljevic,²¹ D. Ferencek,²¹ K. Kadija,²¹ B. Mesic,²¹ A. Starodumov,^{21,h} T. Susa,²¹ M. W. Ather,²² A. Attikis,²² M. Kolosova,²² G. Mavromanolakis,²² J. Mousa,²² C. Nicolaou,²² F. Ptochos,²² P. A. Razis,²² H. Rykaczewski,²² M. Finger,^{23,i} M. Finger Jr.,^{23,i} E. Ayala,²⁴ E. Carrera Jarrin,²⁵ Y. Assran,^{26,j,k} S. Elgammal,^{26,j} S. Khalil,^{26,l} S. Bhowmik,²⁷ A. Carvalho Antunes De Oliveira,²⁷ R. K. Dewanjee,²⁷ K. Ehataht,²⁷ M. Kadastik,²⁷ M. Raidal,²⁷ C. Veelken,²⁷ P. Eerola,²⁸ H. Kirschenmann,²⁸ J. Pekkanen,²⁸ M. Voutilainen,²⁸ J. Havukainen,²⁹ J. K. Heikkilä,²⁹ T. Järvinen,²⁹ V. Karimäki,²⁹ R. Kinnunen,²⁹ T. Lampén,²⁹ K. Lassila-Perini,²⁹ S. Laurila,²⁹ S. Lehti,²⁹ T. Lindén,²⁹ P. Luukka,²⁹ T. Mäenpää,²⁹ H. Siikonen,²⁹ E. Tuominen,²⁹ J. Tuominiemi,²⁹ T. Tuuva,³⁰ M. Besancon,³¹ F. Couderc,³¹ M. Dejardin,³¹ D. Denegri,³¹ J. L. Faure,³¹ F. Ferri,³¹ S. Ganjour,³¹ A. Givernaud,³¹ P. Gras,³¹ G. Hamel de Monchenault,³¹ P. Jarry,³¹ C. Leloup,³¹ E. Locci,³¹ J. Malcles,³¹ G. Negro,³¹ J. Rander,³¹ A. Rosowsky,³¹ M. Ö. Sahin,³¹ M. Titov,³¹ A. Abdulsalam,^{32,m} C. Amendola,³² I. Antropov,³² F. Beaudette,³² P. Busson,³² C. Charlot,³² R. Granier de Cassagnac,³² I. Kucher,³² A. Lobanov,³² J. Martin Blanco,³² M. Nguyen,³² C. Ochando,³² G. Ortona,³² P. Paganini,³² P. Pigard,³² J. Rembser,³² R. Salerno,³² J. B. Sauvan,³² Y. Sirois,³² A. G. Stahl Leitner,³² A. Zabi,³² A. Zghiche,³² J.-L. Agram,^{33,n} J. Andrea,³³ D. Bloch,³³ J.-M. Brom,³³ E. C. Chabert,³³ V. Cherepanov,³³ C. Collard,³³ E. Conte,^{33,n} J.-C. Fontaine,^{33,n} D. Gelé,³³ U. Goerlach,³³ M. Jansová,³³ A.-C. Le Bihan,³³ N. Tonon,³³ P. Van Hove,³³ S. Gadrat,³⁴ S. Beauceron,³⁵ C. Bernet,³⁵ G. Boudoul,³⁵ N. Chanon,³⁵ R. Chierici,³⁵ D. Contardo,³⁵ P. Depasse,³⁵ H. El Mamouni,³⁵ J. Fay,³⁵ L. Finco,³⁵ S. Gascon,³⁵ M. Gouzevitch,³⁵ G. Grenier,³⁵ B. Ille,³⁵ F. Lagarde,³⁵ I. B. Laktineh,³⁵ H. Lattaud,³⁵ M. Lethuillier,³⁵ L. Mirabito,³⁵ S. Perries,³⁵ A. Popov,^{35,o} V. Sordini,³⁵ G. Touquet,³⁵ M. Vander Donckt,³⁵ S. Viret,³⁵ A. Khvedelidze,^{36,i} Z. Tsamalaidze,^{37,i} C. Autermann,³⁸ L. Feld,³⁸ M. K. Kiesel,³⁸ K. Klein,³⁸ M. Lipinski,³⁸ M. Preuten,³⁸ M. P. Rauch,³⁸ C. Schomakers,³⁸ J. Schulz,³⁸ M. Teroerde,³⁸ B. Wittmer,³⁸ V. Zhukov,^{38,o} A. Albert,³⁹ D. Duchardt,³⁹ M. Endres,³⁹ M. Erdmann,³⁹ S. Ghosh,³⁹ A. Güth,³⁹ T. Hebbeker,³⁹ C. Heidemann,³⁹ K. Hoepfner,³⁹ H. Keller,³⁹ L. Mastrolorenzo,³⁹ M. Merschmeyer,³⁹ A. Meyer,³⁹ P. Millet,³⁹ S. Mukherjee,³⁹ T. Pook,³⁹ M. Radziej,³⁹ H. Reithler,³⁹ M. Rieger,³⁹ A. Schmidt,³⁹ D. Teyssier,³⁹ G. Flügge,⁴⁰ O. Hlushchenko,⁴⁰ T. Kress,⁴⁰ A. Künsken,⁴⁰ T. Müller,⁴⁰ A. Nehr Korn,⁴⁰ A. Nowack,⁴⁰ C. Pistone,⁴⁰ O. Pooth,⁴⁰ D. Roy,⁴⁰ H. Sert,⁴⁰ A. Stahl,^{40,p} M. Aldaya Martin,⁴¹ T. Arndt,⁴¹ C. Asawatangtrakuldee,⁴¹ I. Babounikau,⁴¹ K. Beernaert,⁴¹ O. Behnke,⁴¹ U. Behrens,⁴¹ A. Bermúdez Martínez,⁴¹ D. Bertsche,⁴¹ A. A. Bin Anuar,⁴¹ K. Borrás,^{41,q} V. Botta,⁴¹ A. Campbell,⁴¹ P. Connor,⁴¹ C. Contreras-Campana,⁴¹ F. Costanza,⁴¹ V. Danilov,⁴¹ A. De Wit,⁴¹ M. M. Defranchis,⁴¹ C. Diez Pardos,⁴¹ D. Domínguez Damiani,⁴¹ G. Eckerlin,⁴¹ T. Eichhorn,⁴¹ A. Elwood,⁴¹ E. Eren,⁴¹ E. Gallo,^{41,r} A. Geiser,⁴¹ J. M. Grados Luyando,⁴¹ A. Grohsjean,⁴¹ M. Guthoff,⁴¹ M. Haranko,⁴¹ A. Harb,⁴¹ J. Hauk,⁴¹ H. Jung,⁴¹ M. Kasemann,⁴¹ J. Keaveney,⁴¹ C. Kleinwort,⁴¹ J. Knolle,⁴¹ D. Krücker,⁴¹ W. Lange,⁴¹ A. Lelek,⁴¹ T. Lenz,⁴¹ K. Lipka,⁴¹ W. Lohmann,^{41,s} R. Mankel,⁴¹ I.-A. Melzer-Pellmann,⁴¹ A. B. Meyer,⁴¹ M. Meyer,⁴¹ M. Missiroli,⁴¹ G. Mittag,⁴¹ J. Mnich,⁴¹ V. Myronenko,⁴¹ S. K. Pflitsch,⁴¹ D. Pitzl,⁴¹ A. Raspereza,⁴¹ M. Savitskiy,⁴¹ P. Saxena,⁴¹ P. Schütze,⁴¹ C. Schwanenberger,⁴¹ R. Shevchenko,⁴¹ A. Singh,⁴¹ H. Tholen,⁴¹ O. Turkot,⁴¹ A. Vagnerini,⁴¹ G. P. Van Onsem,⁴¹ R. Walsh,⁴¹ Y. Wen,⁴¹ K. Wichmann,⁴¹ C. Wissing,⁴¹ O. Zenaiev,⁴¹ R. Aggleton,⁴² S. Bein,⁴² L. Benato,⁴² A. Benecke,⁴² V. Blobel,⁴² T. Dreyer,⁴² E. Garutti,⁴² D. Gonzalez,⁴² P. Gunnellini,⁴² J. Haller,⁴² A. Hinemann,⁴² A. Karavdina,⁴² G. Kasieczka,⁴² R. Klanner,⁴² R. Kogler,⁴² N. Kovalchuk,⁴² S. Kurz,⁴² V. Kutzner,⁴² J. Lange,⁴² D. Marconi,⁴² J. Multhaupt,⁴² M. Niedziela,⁴² C. E. N. Niemeyer,⁴² D. Nowatschin,⁴² A. Perieanu,⁴²

A. Reimers,⁴² O. Rieger,⁴² C. Scharf,⁴² P. Schleper,⁴² S. Schumann,⁴² J. Schwandt,⁴² J. Sonneveld,⁴² H. Stadie,⁴² G. Steinbrück,⁴² F. M. Stober,⁴² M. Stöver,⁴² A. Vanhoefer,⁴² B. Vormwald,⁴² I. Zoi,⁴² M. Akbiyik,⁴³ C. Barth,⁴³ M. Baselga,⁴³ S. Baur,⁴³ E. Butz,⁴³ R. Caspart,⁴³ T. Chwalek,⁴³ F. Colombo,⁴³ W. De Boer,⁴³ A. Dierlamm,⁴³ K. El Morabit,⁴³ N. Faltermann,⁴³ B. Freund,⁴³ M. Giffels,⁴³ M. A. Harrendorf,⁴³ F. Hartmann,^{43,p} S. M. Heindl,⁴³ U. Husemann,⁴³ F. Kassel,^{43,p} I. Katkov,^{43,o} S. Kudella,⁴³ H. Mildner,⁴³ S. Mitra,⁴³ M. U. Mozer,⁴³ Th. Müller,⁴³ M. Plagge,⁴³ G. Quast,⁴³ K. Rabbertz,⁴³ M. Schröder,⁴³ I. Shvetsov,⁴³ G. Sieber,⁴³ H. J. Simonis,⁴³ R. Ulrich,⁴³ S. Wayand,⁴³ M. Weber,⁴³ T. Weiler,⁴³ S. Williamson,⁴³ C. Wöhrmann,⁴³ R. Wolf,⁴³ G. Anagnostou,⁴⁴ G. Daskalakis,⁴⁴ T. Geralis,⁴⁴ A. Kyriakis,⁴⁴ D. Loukas,⁴⁴ G. Paspalaki,⁴⁴ I. Topsis-Giotis,⁴⁴ G. Karathanasis,⁴⁵ S. Kesisoglou,⁴⁵ P. Kontaxakis,⁴⁵ A. Panagiotou,⁴⁵ I. Papavergou,⁴⁵ N. Saoulidou,⁴⁵ E. Tziaferi,⁴⁵ K. Vellidis,⁴⁵ K. Kousouris,⁴⁶ I. Papakrivopoulos,⁴⁶ G. Tsipolitis,⁴⁶ I. Evangelou,⁴⁷ C. Foudas,⁴⁷ P. Gianneios,⁴⁷ P. Katsoulis,⁴⁷ P. Kokkas,⁴⁷ S. Mallios,⁴⁷ N. Manthos,⁴⁷ I. Papadopoulos,⁴⁷ E. Paradas,⁴⁷ J. Strologas,⁴⁷ F. A. Triantis,⁴⁷ D. Tsitsonis,⁴⁷ M. Bartók,^{48,i} M. Csanad,⁴⁸ N. Filipovic,⁴⁸ P. Major,⁴⁸ M. I. Nagy,⁴⁸ G. Pasztor,⁴⁸ O. Surányi,⁴⁸ G. I. Veres,⁴⁸ G. Bencze,⁴⁹ C. Hajdu,⁴⁹ D. Horvath,^{49,u} Á. Hunyadi,⁴⁹ F. Sikler,⁴⁹ T. Á. Vámi,⁴⁹ V. Veszpremi,⁴⁹ G. Vesztergombi,^{49,a,t} N. Beni,⁵⁰ S. Czellar,⁵⁰ J. Karancsi,^{50,v} A. Makovec,⁵⁰ J. Molnar,⁵⁰ Z. Szillasi,⁵⁰ P. Raics,⁵¹ Z. L. Trocsanyi,⁵¹ B. Ujvari,⁵¹ S. Choudhury,⁵² J. R. Komaragiri,⁵² P. C. Tiwari,⁵² S. Bahinipati,^{53,w} C. Kar,⁵³ P. Mal,⁵³ K. Mandal,⁵³ A. Nayak,^{53,x} D. K. Sahoo,^{53,w} S. K. Swain,⁵³ S. Bansal,⁵⁴ S. B. Beri,⁵⁴ V. Bhatnagar,⁵⁴ S. Chauhan,⁵⁴ R. Chawla,⁵⁴ N. Dhingra,⁵⁴ R. Gupta,⁵⁴ A. Kaur,⁵⁴ M. Kaur,⁵⁴ S. Kaur,⁵⁴ R. Kumar,⁵⁴ P. Kumari,⁵⁴ M. Lohan,⁵⁴ A. Mehta,⁵⁴ K. Sandeep,⁵⁴ S. Sharma,⁵⁴ J. B. Singh,⁵⁴ A. K. Virdi,⁵⁴ G. Walia,⁵⁴ A. Bhardwaj,⁵⁵ B. C. Choudhary,⁵⁵ R. B. Garg,⁵⁵ M. Gola,⁵⁵ S. Keshri,⁵⁵ Ashok Kumar,⁵⁵ S. Malhotra,⁵⁵ M. Naimuddin,⁵⁵ P. Priyanka,⁵⁵ K. Ranjan,⁵⁵ Aashaq Shah,⁵⁵ R. Sharma,⁵⁵ R. Bhardwaj,^{56,y} M. Bharti,⁵⁶ R. Bhattacharya,⁵⁶ S. Bhattacharya,⁵⁶ U. Bhawandeep,^{56,y} D. Bhowmik,⁵⁶ S. Dey,⁵⁶ S. Dutt,^{56,y} S. Dutta,⁵⁶ S. Ghosh,⁵⁶ K. Mondal,⁵⁶ S. Nandan,⁵⁶ A. Purohit,⁵⁶ P. K. Rout,⁵⁶ A. Roy,⁵⁶ S. Roy Chowdhury,⁵⁶ G. Saha,⁵⁶ S. Sarkar,⁵⁶ M. Sharan,⁵⁶ B. Singh,⁵⁶ S. Thakur,^{56,y} P. K. Behera,⁵⁷ R. Chudasama,⁵⁸ D. Dutta,⁵⁸ V. Jha,⁵⁸ V. Kumar,⁵⁸ P. K. Netrakanti,⁵⁸ L. M. Pant,⁵⁸ P. Shukla,⁵⁸ T. Aziz,⁵⁹ M. A. Bhat,⁵⁹ S. Dugad,⁵⁹ G. B. Mohanty,⁵⁹ N. Sur,⁵⁹ B. Sutar,⁵⁹ Ravindra Kumar Verma,⁵⁹ S. Banerjee,⁶⁰ S. Bhattacharya,⁶⁰ S. Chatterjee,⁶⁰ P. Das,⁶⁰ M. Guchait,⁶⁰ Sa. Jain,⁶⁰ S. Karmakar,⁶⁰ S. Kumar,⁶⁰ M. Maity,^{60,z} G. Majumder,⁶⁰ K. Mazumdar,⁶⁰ N. Sahoo,⁶⁰ T. Sarkar,^{60,z} S. Chauhan,⁶¹ S. Dube,⁶¹ V. Hegde,⁶¹ A. Kapoor,⁶¹ K. Kotheekar,⁶¹ S. Pandey,⁶¹ A. Rane,⁶¹ S. Sharma,⁶¹ S. Chenarani,^{62,aa} E. Eskandari Tadavani,⁶² S. M. Etesami,^{62,aa} M. Khakzad,⁶² M. Mohammadi Najafabadi,⁶² M. Naseri,⁶² F. Rezaei Hosseinabadi,⁶² B. Safarzadeh,^{62,bb} M. Zeinali,⁶² M. Felcini,⁶³ M. Grunewald,⁶³ M. Abbrescia,^{64a,64b} C. Calabria,^{64a,64b} A. Colaleo,^{64a} D. Creanza,^{64a,64c} L. Cristella,^{64a,64b} N. De Filippis,^{64a,64c} M. De Palma,^{64a,64b} A. Di Florio,^{64a,64b} F. Errico,^{64a,64b} L. Fiore,^{64a} A. Gelmi,^{64a,64b} G. Iaselli,^{64a,64c} M. Ince,^{64a,64b} S. Lezki,^{64a,64b} G. Maggi,^{64a,64c} M. Maggi,^{64a} G. Miniello,^{64a,64b} S. My,^{64a,64b} S. Nuzzo,^{64a,64b} A. Pompili,^{64a,64b} G. Pugliese,^{64a,64c} R. Radogna,^{64a} A. Ranieri,^{64a} G. Selvaggi,^{64a,64b} A. Sharma,^{64a} L. Silvestris,^{64a} R. Venditti,^{64a} P. Verwilligen,^{64a} G. Zito,^{64a} G. Abbiendi,^{65a} C. Battilana,^{65a,65b} D. Bonacorsi,^{65a,65b} L. Borgonovi,^{65a,65b} S. Braibant-Giacomelli,^{65a,65b} R. Campanini,^{65a,65b} P. Capiluppi,^{65a,65b} A. Castro,^{65a,65b} F. R. Cavallo,^{65a} S. S. Chhibra,^{65a,65b} C. Ciocca,^{65a} G. Codispoti,^{65a,65b} M. Cuffiani,^{65a,65b} G. M. Dallavalle,^{65a} F. Fabbri,^{65a} A. Fanfani,^{65a,65b} P. Giacomelli,^{65a} C. Grandi,^{65a} L. Guiducci,^{65a,65b} S. Lo Meo,^{65a} S. Marcellini,^{65a} G. Masetti,^{65a} A. Montanari,^{65a} F. L. Navarria,^{65a,65b} A. Perrotta,^{65a} F. Primavera,^{65a,65b,p} A. M. Rossi,^{65a,65b} T. Rovelli,^{65a,65b} G. P. Siroli,^{65a,65b} N. Tosi,^{65a} S. Albergo,^{66a,66b} A. Di Mattia,^{66a} R. Potenza,^{66a,66b} A. Tricomi,^{66a,66b} C. Tuve,^{66a,66b} G. Barbagli,^{67a} K. Chatterjee,^{67a,67b} V. Ciulli,^{67a,67b} C. Civinini,^{67a} R. D'Alessandro,^{67a,67b} E. Focardi,^{67a,67b} G. Latino,^{67a} P. Lenzi,^{67a,67b} M. Meschini,^{67a} S. Paoletti,^{67a} L. Russo,^{67a,cc} G. Sguazzoni,^{67a} D. Strom,^{67a} L. Viliani,^{67a} L. Benussi,⁶⁸ S. Bianco,⁶⁸ F. Fabbri,⁶⁸ D. Piccolo,⁶⁸ F. Ferro,^{69a} F. Ravera,^{69a,69b} E. Robutti,^{69a} S. Tosi,^{69a,69b} A. Benaglia,^{70a} A. Beschi,^{70a,70b} L. Brianza,^{70a,70b} F. Brivio,^{70a,70b} V. Ciriolo,^{70a,70b,p} S. Di Guida,^{70a,70b,p} M. E. Dinardo,^{70a,70b} S. Fiorendi,^{70a,70b} S. Gennai,^{70a} A. Ghezzi,^{70a,70b} P. Govoni,^{70a,70b} M. Malberti,^{70a,70b} S. Malvezzi,^{70a} A. Massironi,^{70a,70b} D. Menasce,^{70a} F. Monti,^{70a} L. Moroni,^{70a} M. Paganoni,^{70a,70b} D. Pedrini,^{70a} S. Ragazzi,^{70a,70b} T. Tabarelli de Fatis,^{70a,70b} D. Zuolo,^{70a,70b} S. Buontempo,^{71a} N. Cavallo,^{71a,71c} A. Di Crescenzo,^{71a,71b} F. Fabozzi,^{71a,71c} F. Fienga,^{71a} G. Galati,^{71a} A. O. M. Iorio,^{71a,71b} W. A. Khan,^{71a} L. Lista,^{71a} S. Meola,^{71a,71d,p} P. Paolucci,^{71a,p} C. Sciacca,^{71a,71b} E. Voevodina,^{71a,71b} P. Azzi,^{72a} N. Bacchetta,^{72a} D. Bisello,^{72a,72b} A. Boletti,^{72a,72b} A. Bragagnolo,^{72a} R. Carlin,^{72a,72b} P. Checchia,^{72a} M. Dall'Osso,^{72a,72b} P. De Castro Manzano,^{72a} T. Dorigo,^{72a} U. Dosselli,^{72a} F. Gasparini,^{72a,72b} U. Gasparini,^{72a,72b} A. Gozzelino,^{72a} S. Y. Hoh,^{72a} S. Lacaprara,^{72a} P. Lujan,^{72a} M. Margoni,^{72a,72b} A. T. Meneguzzo,^{72a,72b} J. Pazzini,^{72a,72b} P. Ronchese,^{72a,72b} R. Rossin,^{72a,72b} F. Simonetto,^{72a,72b} A. Tiko,^{72a} E. Torassa,^{72a} M. Zanetti,^{72a,72b} P. Zotto,^{72a,72b} G. Zumerle,^{72a,72b} A. Braghieri,^{73a} A. Magnani,^{73a} P. Montagna,^{73a,73b} S. P. Ratti,^{73a,73b} V. Re,^{73a} M. Ressegotti,^{73a,73b}

C. Riccardi,^{73a,73b} P. Salvini,^{73a} I. Vai,^{73a,73b} P. Vitulo,^{73a,73b} M. Biasini,^{74a,74b} G. M. Bilei,^{74a} C. Cecchi,^{74a,74b}
D. Ciangottini,^{74a,74b} L. Fanò,^{74a,74b} P. Lariccia,^{74a,74b} R. Leonardi,^{74a,74b} E. Manoni,^{74a} G. Mantovani,^{74a,74b} V. Mariani,^{74a,74b}
M. Menichelli,^{74a} A. Rossi,^{74a,74b} A. Santocchia,^{74a,74b} D. Spiga,^{74a} K. Androsov,^{75a} P. Azzurri,^{75a} G. Bagliesi,^{75a}
L. Bianchini,^{75a} T. Boccali,^{75a} L. Borrello,^{75a} R. Castaldi,^{75a} M. A. Ciocci,^{75a,75b} R. Dell'Orso,^{75a} G. Fedi,^{75a} F. Fiori,^{75a,75c}
L. Giannini,^{75a,75c} A. Giassi,^{75a} M. T. Grippo,^{75a} F. Ligabue,^{75a,75c} E. Manca,^{75a,75c} G. Mandorli,^{75a,75c} A. Messineo,^{75a,75b}
F. Palla,^{75a} A. Rizzi,^{75a,75b} P. Spagnolo,^{75a} R. Tenchini,^{75a} G. Tonelli,^{75a,75b} A. Venturi,^{75a} P. G. Verdini,^{75a} L. Barone,^{76a,76b}
F. Cavallari,^{76a} M. Cipriani,^{76a,76b} D. Del Re,^{76a,76b} E. Di Marco,^{76a,76b} M. Diemoz,^{76a} S. Gelli,^{76a,76b} E. Longo,^{76a,76b}
B. Marzocchi,^{76a,76b} P. Meridiani,^{76a} G. Organtini,^{76a,76b} F. Pandolfi,^{76a} R. Paramatti,^{76a,76b} F. Preiato,^{76a,76b} S. Rahatlou,^{76a,76b}
C. Rovelli,^{76a} F. Santanastasio,^{76a,76b} N. Amapane,^{77a,77b} R. Arcidiacono,^{77a,77c} S. Argiro,^{77a,77b} M. Arneodo,^{77a,77c}
N. Bartosik,^{77a} R. Bellan,^{77a,77b} C. Biino,^{77a} N. Cartiglia,^{77a} F. Cenna,^{77a,77b} S. Cometti,^{77a} M. Costa,^{77a,77b} R. Covarelli,^{77a,77b}
N. Demaria,^{77a} B. Kiani,^{77a,77b} C. Mariotti,^{77a} S. Maselli,^{77a} E. Migliore,^{77a,77b} V. Monaco,^{77a,77b} E. Monteil,^{77a,77b}
M. Monteno,^{77a} M. M. Obertino,^{77a,77b} L. Pacher,^{77a,77b} N. Pastrone,^{77a} M. Pelliccioni,^{77a} G. L. Pinna Angioni,^{77a,77b}
A. Romero,^{77a,77b} M. Ruspa,^{77a,77c} R. Sacchi,^{77a,77b} K. Shchelina,^{77a,77b} V. Sola,^{77a} A. Solano,^{77a,77b} D. Soldi,^{77a,77b}
A. Staiano,^{77a} S. Belforte,^{78a} V. Candelise,^{78a,78b} M. Casarsa,^{78a} F. Cossutti,^{78a} A. Da Rold,^{78a,78b} G. Della Ricca,^{78a,78b}
F. Vazzoler,^{78a,78b} A. Zanetti,^{78a} D. H. Kim,⁷⁹ G. N. Kim,⁷⁹ M. S. Kim,⁷⁹ J. Lee,⁷⁹ S. Lee,⁷⁹ S. W. Lee,⁷⁹ C. S. Moon,⁷⁹
Y. D. Oh,⁷⁹ S. Sekmen,⁷⁹ D. C. Son,⁷⁹ Y. C. Yang,⁷⁹ H. Kim,⁸⁰ D. H. Moon,⁸⁰ G. Oh,⁸⁰ J. Goh,^{81,dd} T. J. Kim,⁸¹ S. Cho,⁸²
S. Choi,⁸² Y. Go,⁸² D. Gyun,⁸² S. Ha,⁸² B. Hong,⁸² Y. Jo,⁸² K. Lee,⁸² K. S. Lee,⁸² S. Lee,⁸² J. Lim,⁸² S. K. Park,⁸² Y. Roh,⁸²
H. S. Kim,⁸³ J. Almond,⁸⁴ J. Kim,⁸⁴ J. S. Kim,⁸⁴ H. Lee,⁸⁴ K. Lee,⁸⁴ K. Nam,⁸⁴ S. B. Oh,⁸⁴ B. C. Radburn-Smith,⁸⁴
S. h. Seo,⁸⁴ U. K. Yang,⁸⁴ H. D. Yoo,⁸⁴ G. B. Yu,⁸⁴ D. Jeon,⁸⁵ H. Kim,⁸⁵ J. H. Kim,⁸⁵ J. S. H. Lee,⁸⁵ I. C. Park,⁸⁵ Y. Choi,⁸⁶
C. Hwang,⁸⁶ J. Lee,⁸⁶ I. Yu,⁸⁶ V. Dudenias,⁸⁷ A. Juodagalvis,⁸⁷ J. Vaitkus,⁸⁷ I. Ahmed,⁸⁸ Z. A. Ibrahim,⁸⁸
M. A. B. Md Ali,^{88,ee} F. Mohamad Idris,^{88,ff} W. A. T. Wan Abdullah,⁸⁸ M. N. Yusli,⁸⁸ Z. Zolkapli,⁸⁸ J. F. Benitez,⁸⁹
A. Castaneda Hernandez,⁸⁹ J. A. Murillo Quijada,⁸⁹ H. Castilla-Valdez,⁹⁰ E. De La Cruz-Burelo,⁹⁰ M. C. Duran-Osuna,⁹⁰
I. Heredia-De La Cruz,^{90,gg} R. Lopez-Fernandez,⁹⁰ J. Mejia Guisao,⁹⁰ R. I. Rabadan-Trejo,⁹⁰ M. Ramirez-Garcia,⁹⁰
G. Ramirez-Sanchez,⁹⁰ R. Reyes-Almanza,⁹⁰ A. Sanchez-Hernandez,⁹⁰ S. Carrillo Moreno,⁹¹ C. Oropeza Barrera,⁹¹
F. Vazquez Valencia,⁹¹ J. Eysermans,⁹² I. Pedraza,⁹² H. A. Salazar Ibarguen,⁹² C. Uribe Estrada,⁹² A. Morelos Pineda,⁹³
D. Krofcheck,⁹⁴ S. Bheesette,⁹⁵ P. H. Butler,⁹⁵ A. Ahmad,⁹⁶ M. Ahmad,⁹⁶ M. I. Asghar,⁹⁶ Q. Hassan,⁹⁶ H. R. Hoorani,⁹⁶
A. Saddique,⁹⁶ M. A. Shah,⁹⁶ M. Shoaib,⁹⁶ M. Waqas,⁹⁶ H. Bialkowska,⁹⁷ M. Bluj,⁹⁷ B. Boimska,⁹⁷ T. Frueboes,⁹⁷
M. Górski,⁹⁷ M. Kazana,⁹⁷ K. Nawrocki,⁹⁷ M. Szleper,⁹⁷ P. Traczyk,⁹⁷ P. Zalewski,⁹⁷ K. Bunkowski,⁹⁸ A. Byszk,^{98,hh}
K. Doroba,⁹⁸ A. Kalinowski,⁹⁸ M. Konecki,⁹⁸ J. Krolikowski,⁹⁸ M. Misiura,⁹⁸ M. Olszewski,⁹⁸ A. Pyskir,⁹⁸ M. Walczak,⁹⁸
M. Araujo,⁹⁹ P. Bargassa,⁹⁹ C. Beirão Da Cruz E Silva,⁹⁹ A. Di Francesco,⁹⁹ P. Faccioli,⁹⁹ B. Galinhas,⁹⁹ M. Gallinaro,⁹⁹
J. Hollar,⁹⁹ N. Leonardo,⁹⁹ M. V. Nemallapudi,⁹⁹ J. Seixas,⁹⁹ G. Strong,⁹⁹ O. Toldaiev,⁹⁹ D. Vadrucio,⁹⁹ J. Varela,⁹⁹
S. Afanasiev,¹⁰⁰ P. Bunin,¹⁰⁰ M. Gavrilenko,¹⁰⁰ I. Golutvin,¹⁰⁰ I. Gorbunov,¹⁰⁰ A. Kamenev,¹⁰⁰ V. Karjavine,¹⁰⁰ A. Lanev,¹⁰⁰
A. Malakhov,¹⁰⁰ V. Matveev,^{100,ii,jj} P. Moiseenz,¹⁰⁰ V. Palichik,¹⁰⁰ V. Perelygin,¹⁰⁰ S. Shmatov,¹⁰⁰ S. Shulha,¹⁰⁰
N. Skatchkov,¹⁰⁰ V. Smirnov,¹⁰⁰ N. Voytishin,¹⁰⁰ A. Zarubin,¹⁰⁰ V. Golovtsov,¹⁰¹ Y. Ivanov,¹⁰¹ V. Kim,^{101,kk}
E. Kuznetsova,^{101,ll} P. Levchenko,¹⁰¹ V. Murzin,¹⁰¹ V. Oreshkin,¹⁰¹ I. Smirnov,¹⁰¹ D. Sosnov,¹⁰¹ V. Sulimov,¹⁰¹ L. Uvarov,¹⁰¹
S. Vavilov,¹⁰¹ A. Vorobyev,¹⁰¹ Yu. Andreev,¹⁰² A. Dermenev,¹⁰² S. Gninenko,¹⁰² N. Golubev,¹⁰² A. Karneyeu,¹⁰²
M. Kirsanov,¹⁰² N. Krasnikov,¹⁰² A. Pashenkov,¹⁰² D. Tlisov,¹⁰² A. Toropin,¹⁰² V. Epshteyn,¹⁰³ V. Gavrillov,¹⁰³
N. Lychkovskaya,¹⁰³ V. Popov,¹⁰³ I. Pozdnyakov,¹⁰³ G. Safronov,¹⁰³ A. Spiridonov,¹⁰³ A. Stepenov,¹⁰³ V. Stolin,¹⁰³
M. Toms,¹⁰³ E. Vlasov,¹⁰³ A. Zhokin,¹⁰³ T. Aushev,¹⁰⁴ R. Chistov,^{105,mmm} M. Danilov,^{105,mmm} P. Parygin,¹⁰⁵ D. Philippov,¹⁰⁵
S. Polikarpov,^{105,mmm} E. Tarkovskii,¹⁰⁵ V. Andreev,¹⁰⁶ M. Azarkin,^{106,jj} I. Dremin,^{106,jj} M. Kirakosyan,^{106,jj} S. V. Rusakov,¹⁰⁶
A. Terkulov,¹⁰⁶ A. Baskakov,¹⁰⁷ A. Belyaev,¹⁰⁷ E. Boos,¹⁰⁷ M. Dubinin,^{107,nn} L. Dudko,¹⁰⁷ A. Ershov,¹⁰⁷ A. Gribushin,¹⁰⁷
V. Klyukhin,¹⁰⁷ O. Kodolova,¹⁰⁷ I. Lokhtin,¹⁰⁷ I. Miagkov,¹⁰⁷ S. Obraztsov,¹⁰⁷ S. Petrushanko,¹⁰⁷ V. Savrin,¹⁰⁷
A. Snigirev,¹⁰⁷ A. Barnyakov,^{108,oo} V. Blinov,^{108,oo} T. Dimova,^{108,oo} L. Kardapoltsev,^{108,oo} Y. Skovpen,^{108,oo} I. Azhgirey,¹⁰⁹
I. Bayshev,¹⁰⁹ S. Bitiukov,¹⁰⁹ D. Elumakhov,¹⁰⁹ A. Godizov,¹⁰⁹ V. Kachanov,¹⁰⁹ A. Kalinin,¹⁰⁹ D. Konstantinov,¹⁰⁹
P. Mandrik,¹⁰⁹ V. Petrov,¹⁰⁹ R. Ryutin,¹⁰⁹ S. Slabospitskii,¹⁰⁹ A. Sobol,¹⁰⁹ S. Troshin,¹⁰⁹ N. Tyurin,¹⁰⁹ A. Uzunian,¹⁰⁹
A. Volkov,¹⁰⁹ A. Babaev,¹¹⁰ S. Baidali,¹¹⁰ V. Okhotnikov,¹¹⁰ P. Adzic,^{111,pp} P. Cirkovic,¹¹¹ D. Devetak,¹¹¹ M. Dordevic,¹¹¹
J. Milosevic,¹¹¹ J. Alcaraz Maestre,¹¹² A. Álvarez Fernández,¹¹² I. Bachiller,¹¹² M. Barrio Luna,¹¹²
J. A. Brochero Cifuentes,¹¹² M. Cerrada,¹¹² N. Colino,¹¹² B. De La Cruz,¹¹² A. Delgado Peris,¹¹² C. Fernandez Bedoya,¹¹²
J. P. Fernández Ramos,¹¹² J. Flix,¹¹² M. C. Fouz,¹¹² O. Gonzalez Lopez,¹¹² S. Goy Lopez,¹¹² J. M. Hernandez,¹¹²

M. I. Josa,¹¹² D. Moran,¹¹² A. Pérez-Calero Yzquierdo,¹¹² J. Puerta Pelayo,¹¹² I. Redondo,¹¹² L. Romero,¹¹² M. S. Soares,¹¹² A. Triossi,¹¹² C. Albajar,¹¹³ J. F. de Trocóniz,¹¹³ J. Cuevas,¹¹⁴ C. Erice,¹¹⁴ J. Fernandez Menendez,¹¹⁴ S. Folgueras,¹¹⁴ I. Gonzalez Caballero,¹¹⁴ J. R. González Fernández,¹¹⁴ E. Palencia Cortezon,¹¹⁴ V. Rodríguez Bouza,¹¹⁴ S. Sanchez Cruz,¹¹⁴ P. Vischia,¹¹⁴ J. M. Vizán García,¹¹⁴ I. J. Cabrillo,¹¹⁵ A. Calderon,¹¹⁵ B. Chazin Quero,¹¹⁵ J. Duarte Campderros,¹¹⁵ M. Fernandez,¹¹⁵ P. J. Fernández Manteca,¹¹⁵ A. García Alonso,¹¹⁵ J. Garcia-Ferrero,¹¹⁵ G. Gomez,¹¹⁵ A. Lopez Virto,¹¹⁵ J. Marco,¹¹⁵ C. Martínez Rivero,¹¹⁵ P. Martínez Ruiz del Arbol,¹¹⁵ F. Matorras,¹¹⁵ J. Piedra Gomez,¹¹⁵ C. Prieels,¹¹⁵ T. Rodrigo,¹¹⁵ A. Ruiz-Jimeno,¹¹⁵ L. Scodellaro,¹¹⁵ N. Trevisani,¹¹⁵ I. Vila,¹¹⁵ R. Vilar Cortabitarte,¹¹⁵ N. Wickramage,¹¹⁶ D. Abbaneo,¹¹⁷ B. Akgun,¹¹⁷ E. Auffray,¹¹⁷ G. Auzinger,¹¹⁷ P. Baillon,¹¹⁷ A. H. Ball,¹¹⁷ D. Barney,¹¹⁷ J. Bendavid,¹¹⁷ M. Bianco,¹¹⁷ A. Bocci,¹¹⁷ C. Botta,¹¹⁷ E. Brondolin,¹¹⁷ T. Camporesi,¹¹⁷ M. Cepeda,¹¹⁷ G. Cerminara,¹¹⁷ E. Chapon,¹¹⁷ Y. Chen,¹¹⁷ G. Cucciati,¹¹⁷ D. d'Enterria,¹¹⁷ A. Dabrowski,¹¹⁷ N. Daci,¹¹⁷ V. Daponte,¹¹⁷ A. David,¹¹⁷ A. De Roeck,¹¹⁷ N. Deelen,¹¹⁷ M. Dobson,¹¹⁷ M. Dünser,¹¹⁷ N. Dupont,¹¹⁷ A. Elliott-Peisert,¹¹⁷ P. Everaerts,¹¹⁷ F. Fallavollita,^{117,qq} D. Fasanella,¹¹⁷ G. Franzoni,¹¹⁷ J. Fulcher,¹¹⁷ W. Funk,¹¹⁷ D. Gigi,¹¹⁷ A. Gilbert,¹¹⁷ K. Gill,¹¹⁷ F. Glege,¹¹⁷ M. Guilbaud,¹¹⁷ D. Gulhan,¹¹⁷ J. Hegeman,¹¹⁷ C. Heidegger,¹¹⁷ V. Innocente,¹¹⁷ A. Jafari,¹¹⁷ P. Janot,¹¹⁷ O. Karacheban,^{117,s} J. Kieseler,¹¹⁷ A. Kornmayer,¹¹⁷ M. Krammer,^{117,b} C. Lange,¹¹⁷ P. Lecoq,¹¹⁷ C. Lourenço,¹¹⁷ L. Malgeri,¹¹⁷ M. Mannelli,¹¹⁷ F. Meijers,¹¹⁷ J. A. Merlin,¹¹⁷ S. Mersi,¹¹⁷ E. Meschi,¹¹⁷ P. Milenovic,^{117,rr} F. Moortgat,¹¹⁷ M. Mulders,¹¹⁷ J. Ngadiuba,¹¹⁷ S. Nourbakhsh,¹¹⁷ S. Orfanelli,¹¹⁷ L. Orsini,¹¹⁷ F. Pantaleo,^{117,p} L. Pape,¹¹⁷ E. Perez,¹¹⁷ M. Peruzzi,¹¹⁷ A. Petrilli,¹¹⁷ G. Petrucciani,¹¹⁷ A. Pfeiffer,¹¹⁷ M. Pierini,¹¹⁷ F. M. Pitters,¹¹⁷ D. Rabady,¹¹⁷ A. Racz,¹¹⁷ T. Reis,¹¹⁷ G. Rolandi,^{117,ss} M. Rovere,¹¹⁷ H. Sakulin,¹¹⁷ C. Schäfer,¹¹⁷ C. Schwick,¹¹⁷ M. Seidel,¹¹⁷ M. Selvaggi,¹¹⁷ A. Sharma,¹¹⁷ P. Silva,¹¹⁷ P. Sphicas,^{117,tt} A. Stakia,¹¹⁷ J. Steggemann,¹¹⁷ M. Tosi,¹¹⁷ D. Treille,¹¹⁷ A. Tsiros,¹¹⁷ V. Veckalns,^{117,uu} M. Verzetti,¹¹⁷ W. D. Zeuner,¹¹⁷ L. Caminada,^{118,vv} K. Deiters,¹¹⁸ W. Erdmann,¹¹⁸ R. Horisberger,¹¹⁸ Q. Ingram,¹¹⁸ H. C. Kaestli,¹¹⁸ D. Kotlinski,¹¹⁸ U. Langenegger,¹¹⁸ T. Rohe,¹¹⁸ S. A. Wiederkehr,¹¹⁸ M. Backhaus,¹¹⁹ L. Bäni,¹¹⁹ P. Berger,¹¹⁹ N. Chernyavskaya,¹¹⁹ G. Dissertori,¹¹⁹ M. Dittmar,¹¹⁹ M. Donegà,¹¹⁹ C. Dorfer,¹¹⁹ T. A. Gómez Espinosa,¹¹⁹ C. Grab,¹¹⁹ D. Hits,¹¹⁹ J. Hoss,¹¹⁹ T. Klijnsma,¹¹⁹ W. Lustermann,¹¹⁹ R. A. Manzoni,¹¹⁹ M. Marionneau,¹¹⁹ M. T. Meinhard,¹¹⁹ F. Micheli,¹¹⁹ P. Musella,¹¹⁹ F. Nessi-Tedaldi,¹¹⁹ J. Pata,¹¹⁹ F. Pauss,¹¹⁹ G. Perrin,¹¹⁹ L. Perrozzi,¹¹⁹ S. Pigazzini,¹¹⁹ M. Quittnat,¹¹⁹ D. Ruini,¹¹⁹ D. A. Sanz Becerra,¹¹⁹ M. Schönberger,¹¹⁹ L. Shchutska,¹¹⁹ V. R. Tavolaro,¹¹⁹ K. Theofilatos,¹¹⁹ M. L. Vesterbacka Olsson,¹¹⁹ R. Wallny,¹¹⁹ D. H. Zhu,¹¹⁹ T. K. Aarrestad,¹²⁰ C. AMSler,^{120,ww} D. Brzhechko,¹²⁰ M. F. Canelli,¹²⁰ A. De Cosa,¹²⁰ R. Del Burgo,¹²⁰ S. Donato,¹²⁰ C. Galloni,¹²⁰ T. Hreus,¹²⁰ B. Kilminster,¹²⁰ S. Leontsinis,¹²⁰ I. Neutelings,¹²⁰ D. Pinna,¹²⁰ G. Rauco,¹²⁰ P. Robmann,¹²⁰ D. Salerno,¹²⁰ K. Schweiger,¹²⁰ C. Seitz,¹²⁰ Y. Takahashi,¹²⁰ A. Zucchetta,¹²⁰ Y. H. Chang,¹²¹ K. y. Cheng,¹²¹ T. H. Doan,¹²¹ Sh. Jain,¹²¹ R. Khurana,¹²¹ C. M. Kuo,¹²¹ W. Lin,¹²¹ A. Pozdnyakov,¹²¹ S. S. Yu,¹²¹ P. Chang,¹²² Y. Chao,¹²² K. F. Chen,¹²² P. H. Chen,¹²² W.-S. Hou,¹²² Arun Kumar,¹²² Y. F. Liu,¹²² R.-S. Lu,¹²² E. Paganis,¹²² A. Psallidas,¹²² A. Steen,¹²² B. Asavapibhop,¹²³ N. Srimanobhas,¹²³ N. Suwonjandee,¹²³ A. Bat,¹²⁴ F. Boran,¹²⁴ S. Cerci,^{124,xx} S. Damarseckin,¹²⁴ Z. S. Demiroglu,¹²⁴ F. Dolek,¹²⁴ C. Dozen,¹²⁴ I. Dumanoglu,¹²⁴ S. Girgis,¹²⁴ G. Gokbulut,¹²⁴ Y. Guler,¹²⁴ E. Gurpinar,¹²⁴ I. Hos,^{124,yy} C. Isik,¹²⁴ E. E. Kangal,^{124,zz} O. Kara,¹²⁴ A. Kayis Topaksu,¹²⁴ U. Kiminsu,¹²⁴ M. Oglakci,¹²⁴ G. Onengut,¹²⁴ K. Ozdemir,^{124,aaa} S. Ozturk,^{124,bbb} D. Sunar Cerci,^{124,xx} B. Tali,^{124,xx} U. G. Tok,¹²⁴ S. Turkcapar,¹²⁴ I. S. Zorbakir,¹²⁴ C. Zorbilmez,¹²⁴ B. Isildak,^{125,ccc} G. Karapinar,^{125,ddd} M. Yalvac,¹²⁵ M. Zeyrek,¹²⁵ I. O. Atakisi,¹²⁶ E. Gülmez,¹²⁶ M. Kaya,^{126,eee} O. Kaya,^{126,fff} S. Ozkorucuklu,^{126,ggg} S. Tekten,¹²⁶ E. A. Yetkin,^{126,hhh} M. N. Agaras,¹²⁷ A. Cakir,¹²⁷ K. Cankocak,¹²⁷ Y. Komurcu,¹²⁷ S. Sen,^{127,iii} B. Grynyov,¹²⁸ L. Levchuk,¹²⁹ F. Ball,¹³⁰ L. Beck,¹³⁰ J. J. Brooke,¹³⁰ D. Burns,¹³⁰ E. Clement,¹³⁰ D. Cussans,¹³⁰ O. Davignon,¹³⁰ H. Flacher,¹³⁰ J. Goldstein,¹³⁰ G. P. Heath,¹³⁰ H. F. Heath,¹³⁰ L. Kreczko,¹³⁰ D. M. Newbold,^{130,jjj} S. Paramesvaran,¹³⁰ B. Penning,¹³⁰ T. Sakuma,¹³⁰ D. Smith,¹³⁰ V. J. Smith,¹³⁰ J. Taylor,¹³⁰ A. Titterton,¹³⁰ K. W. Bell,¹³¹ A. Belyaev,^{131,kkk} C. Brew,¹³¹ R. M. Brown,¹³¹ D. Cieri,¹³¹ D. J. A. Cockerill,¹³¹ J. A. Coughlan,¹³¹ K. Harder,¹³¹ S. Harper,¹³¹ J. Linacre,¹³¹ E. Olaiya,¹³¹ D. Petyt,¹³¹ C. H. Shepherd-Themistocleous,¹³¹ A. Thea,¹³¹ I. R. Tomalin,¹³¹ T. Williams,¹³¹ W. J. Womersley,¹³¹ R. Bainbridge,¹³² P. Bloch,¹³² J. Borg,¹³² S. Breeze,¹³² O. Buchmuller,¹³² A. Bundock,¹³² S. Casasso,¹³² D. Colling,¹³² P. Dauncey,¹³² G. Davies,¹³² M. Della Negra,¹³² R. Di Maria,¹³² Y. Haddad,¹³² G. Hall,¹³² G. Iles,¹³² T. James,¹³² M. Komm,¹³² C. Laner,¹³² L. Lyons,¹³² A.-M. Magnan,¹³² S. Malik,¹³² A. Martelli,¹³² J. Nash,^{132,lll} A. Nikitenko,^{132,h} V. Palladino,¹³² M. Pesaresi,¹³² A. Richards,¹³² A. Rose,¹³² E. Scott,¹³² C. Seez,¹³² A. Shtipliyski,¹³² G. Singh,¹³² M. Stoye,¹³² T. Strebler,¹³² S. Summers,¹³² A. Tapper,¹³² K. Uchida,¹³² T. Virdee,^{132,p} N. Wardle,¹³² D. Winterbottom,¹³² J. Wright,¹³² S. C. Zenz,¹³² J. E. Cole,¹³³ P. R. Hobson,¹³³ A. Khan,¹³³ P. Kyberd,¹³³ C. K. Mackay,¹³³ A. Morton,¹³³ I. D. Reid,¹³³ L. Teodorescu,¹³³ S. Zahid,¹³³ K. Call,¹³⁴ J. Dittmann,¹³⁴ K. Hatakeyama,¹³⁴

H. Liu,¹³⁴ C. Madrid,¹³⁴ B. McMaster,¹³⁴ N. Pastika,¹³⁴ C. Smith,¹³⁴ R. Bartek,¹³⁵ A. Dominguez,¹³⁵ A. Buccilli,¹³⁶
 S. I. Cooper,¹³⁶ C. Henderson,¹³⁶ P. Rumerio,¹³⁶ C. West,¹³⁶ D. Arcaro,¹³⁷ T. Bose,¹³⁷ D. Gastler,¹³⁷ D. Rankin,¹³⁷
 C. Richardson,¹³⁷ J. Rohlf,¹³⁷ L. Sulak,¹³⁷ D. Zou,¹³⁷ G. Benelli,¹³⁸ X. Coubez,¹³⁸ D. Cutts,¹³⁸ M. Hadley,¹³⁸ J. Hakala,¹³⁸
 U. Heintz,¹³⁸ J. M. Hogan,^{138,mmm} K. H. M. Kwok,¹³⁸ E. Laird,¹³⁸ G. Landsberg,¹³⁸ J. Lee,¹³⁸ Z. Mao,¹³⁸ M. Narain,¹³⁸
 S. Sagir,^{138,nnn} R. Syarif,¹³⁸ E. Usai,¹³⁸ D. Yu,¹³⁸ R. Band,¹³⁹ C. Brainerd,¹³⁹ R. Breedon,¹³⁹ D. Burns,¹³⁹
 M. Calderon De La Barca Sanchez,¹³⁹ M. Chertok,¹³⁹ J. Conway,¹³⁹ R. Conway,¹³⁹ P. T. Cox,¹³⁹ R. Erbacher,¹³⁹ C. Flores,¹³⁹
 G. Funk,¹³⁹ W. Ko,¹³⁹ O. Kukral,¹³⁹ R. Lander,¹³⁹ M. Mulhearn,¹³⁹ D. Pellett,¹³⁹ J. Pilot,¹³⁹ S. Shalhout,¹³⁹ M. Shi,¹³⁹
 D. Stolp,¹³⁹ D. Taylor,¹³⁹ K. Tos,¹³⁹ M. Tripathi,¹³⁹ Z. Wang,¹³⁹ F. Zhang,¹³⁹ M. Bachtis,¹⁴⁰ C. Bravo,¹⁴⁰ R. Cousins,¹⁴⁰
 A. Dasgupta,¹⁴⁰ A. Florent,¹⁴⁰ J. Hauser,¹⁴⁰ M. Ignatenko,¹⁴⁰ N. Mccoll,¹⁴⁰ S. Regnard,¹⁴⁰ D. Saltzberg,¹⁴⁰ C. Schnaible,¹⁴⁰
 V. Valuev,¹⁴⁰ E. Bouvier,¹⁴¹ K. Burt,¹⁴¹ R. Clare,¹⁴¹ J. W. Gary,¹⁴¹ S. M. A. Ghiasi Shirazi,¹⁴¹ G. Hanson,¹⁴¹
 G. Karapostoli,¹⁴¹ E. Kennedy,¹⁴¹ F. Lacroix,¹⁴¹ O. R. Long,¹⁴¹ M. Olmedo Negrete,¹⁴¹ M. I. Paneva,¹⁴¹ W. Si,¹⁴¹
 L. Wang,¹⁴¹ H. Wei,¹⁴¹ S. Wimpenny,¹⁴¹ B. R. Yates,¹⁴¹ J. G. Branson,¹⁴² P. Chang,¹⁴² S. Cittolin,¹⁴² M. Derdzinski,¹⁴²
 R. Gerosa,¹⁴² D. Gilbert,¹⁴² B. Hashemi,¹⁴² A. Holzner,¹⁴² D. Klein,¹⁴² G. Kole,¹⁴² V. Krutelyov,¹⁴² J. Letts,¹⁴²
 M. Masciovecchio,¹⁴² D. Olivito,¹⁴² S. Padhi,¹⁴² M. Pieri,¹⁴² M. Sani,¹⁴² V. Sharma,¹⁴² S. Simon,¹⁴² M. Tadel,¹⁴²
 A. Vartak,¹⁴² S. Wasserbaech,^{142,ooo} J. Wood,¹⁴² F. Würthwein,¹⁴² A. Yagil,¹⁴² G. Zevi Della Porta,¹⁴² N. Amin,¹⁴³
 R. Bhandari,¹⁴³ J. Bradmiller-Feld,¹⁴³ C. Campagnari,¹⁴³ M. Citron,¹⁴³ A. Dishaw,¹⁴³ V. Dutta,¹⁴³ M. Franco Sevilla,¹⁴³
 L. Gouskos,¹⁴³ R. Heller,¹⁴³ J. Incandela,¹⁴³ A. Ovcharova,¹⁴³ H. Qu,¹⁴³ J. Richman,¹⁴³ D. Stuart,¹⁴³ I. Suarez,¹⁴³ S. Wang,¹⁴³
 J. Yoo,¹⁴³ D. Anderson,¹⁴⁴ A. Bornheim,¹⁴⁴ J. M. Lawhorn,¹⁴⁴ H. B. Newman,¹⁴⁴ T. Q. Nguyen,¹⁴⁴ M. Spiropulu,¹⁴⁴
 J. R. Vlimant,¹⁴⁴ R. Wilkinson,¹⁴⁴ S. Xie,¹⁴⁴ Z. Zhang,¹⁴⁴ R. Y. Zhu,¹⁴⁴ M. B. Andrews,¹⁴⁵ T. Ferguson,¹⁴⁵ T. Mudholkar,¹⁴⁵
 M. Paulini,¹⁴⁵ M. Sun,¹⁴⁵ I. Vorobiev,¹⁴⁵ M. Weinberg,¹⁴⁵ J. P. Cumalat,¹⁴⁶ W. T. Ford,¹⁴⁶ F. Jensen,¹⁴⁶ A. Johnson,¹⁴⁶
 M. Krohn,¹⁴⁶ E. MacDonald,¹⁴⁶ T. Mulholland,¹⁴⁶ R. Patel,¹⁴⁶ K. Stenson,¹⁴⁶ K. A. Ulmer,¹⁴⁶ S. R. Wagner,¹⁴⁶
 J. Alexander,¹⁴⁷ J. Chaves,¹⁴⁷ Y. Cheng,¹⁴⁷ J. Chu,¹⁴⁷ A. Datta,¹⁴⁷ K. Mcdermott,¹⁴⁷ N. Mirman,¹⁴⁷ J. R. Patterson,¹⁴⁷
 D. Quach,¹⁴⁷ A. Rinkevicius,¹⁴⁷ A. Ryd,¹⁴⁷ L. Skinnari,¹⁴⁷ L. Soffi,¹⁴⁷ S. M. Tan,¹⁴⁷ Z. Tao,¹⁴⁷ J. Thom,¹⁴⁷ J. Tucker,¹⁴⁷
 P. Wittich,¹⁴⁷ M. Zientek,¹⁴⁷ S. Abdullin,¹⁴⁸ M. Albrow,¹⁴⁸ M. Alyari,¹⁴⁸ G. Apollinari,¹⁴⁸ A. Apresyan,¹⁴⁸ A. Apyan,¹⁴⁸
 S. Banerjee,¹⁴⁸ L. A. T. Bauerdick,¹⁴⁸ A. Beretvas,¹⁴⁸ J. Berryhill,¹⁴⁸ P. C. Bhat,¹⁴⁸ G. Bolla,^{148,a} K. Burkett,¹⁴⁸
 J. N. Butler,¹⁴⁸ A. Canepa,¹⁴⁸ G. B. Cerati,¹⁴⁸ H. W. K. Cheung,¹⁴⁸ F. Chlebana,¹⁴⁸ M. Cremonesi,¹⁴⁸ J. Duarte,¹⁴⁸
 V. D. Elvira,¹⁴⁸ J. Freeman,¹⁴⁸ Z. Gece,¹⁴⁸ E. Gottschalk,¹⁴⁸ L. Gray,¹⁴⁸ D. Green,¹⁴⁸ S. Grünendahl,¹⁴⁸ O. Gutsche,¹⁴⁸
 J. Hanlon,¹⁴⁸ R. M. Harris,¹⁴⁸ S. Hasegawa,¹⁴⁸ J. Hirschauer,¹⁴⁸ Z. Hu,¹⁴⁸ B. Jayatilaka,¹⁴⁸ S. Jindariani,¹⁴⁸ M. Johnson,¹⁴⁸
 U. Joshi,¹⁴⁸ B. Klima,¹⁴⁸ M. J. Kortelainen,¹⁴⁸ B. Kreis,¹⁴⁸ S. Lammel,¹⁴⁸ D. Lincoln,¹⁴⁸ R. Lipton,¹⁴⁸ M. Liu,¹⁴⁸ T. Liu,¹⁴⁸
 J. Lykken,¹⁴⁸ K. Maeshima,¹⁴⁸ J. M. Marraffino,¹⁴⁸ D. Mason,¹⁴⁸ P. McBride,¹⁴⁸ P. Merkel,¹⁴⁸ S. Mrenna,¹⁴⁸ S. Nahn,¹⁴⁸
 V. O'Dell,¹⁴⁸ K. Pedro,¹⁴⁸ C. Pena,¹⁴⁸ O. Prokofyev,¹⁴⁸ G. Rakness,¹⁴⁸ L. Ristori,¹⁴⁸ A. Savoy-Navarro,^{148,ppp}
 B. Schneider,¹⁴⁸ E. Sexton-Kennedy,¹⁴⁸ A. Soha,¹⁴⁸ W. J. Spalding,¹⁴⁸ L. Spiegel,¹⁴⁸ S. Stoynev,¹⁴⁸ J. Strait,¹⁴⁸ N. Strobbe,¹⁴⁸
 L. Taylor,¹⁴⁸ S. Tkaczyk,¹⁴⁸ N. V. Tran,¹⁴⁸ L. Uplegger,¹⁴⁸ E. W. Vaandering,¹⁴⁸ C. Vernieri,¹⁴⁸ M. Verzocchi,¹⁴⁸ R. Vidal,¹⁴⁸
 M. Wang,¹⁴⁸ H. A. Weber,¹⁴⁸ A. Whitbeck,¹⁴⁸ D. Acosta,¹⁴⁹ P. Avery,¹⁴⁹ P. Bortignon,¹⁴⁹ D. Bourilkov,¹⁴⁹ A. Brinkerhoff,¹⁴⁹
 L. Cadamuro,¹⁴⁹ A. Carnes,¹⁴⁹ M. Carver,¹⁴⁹ D. Curry,¹⁴⁹ R. D. Field,¹⁴⁹ S. V. Gleyzer,¹⁴⁹ B. M. Joshi,¹⁴⁹ J. Konigsberg,¹⁴⁹
 A. Korytov,¹⁴⁹ K. H. Lo,¹⁴⁹ P. Ma,¹⁴⁹ K. Matchev,¹⁴⁹ H. Mei,¹⁴⁹ G. Mitselmakher,¹⁴⁹ D. Rosenzweig,¹⁴⁹ K. Shi,¹⁴⁹
 D. Sperka,¹⁴⁹ J. Wang,¹⁴⁹ S. Wang,¹⁴⁹ Y. R. Joshi,¹⁵⁰ S. Linn,¹⁵⁰ A. Ackert,¹⁵¹ T. Adams,¹⁵¹ A. Askew,¹⁵¹ S. Hagopian,¹⁵¹
 V. Hagopian,¹⁵¹ K. F. Johnson,¹⁵¹ T. Kolberg,¹⁵¹ G. Martinez,¹⁵¹ T. Perry,¹⁵¹ H. Prosper,¹⁵¹ A. Saha,¹⁵¹ C. Schiber,¹⁵¹
 V. Sharma,¹⁵¹ R. Yohay,¹⁵¹ M. M. Baarmand,¹⁵² V. Bhopatkar,¹⁵² S. Colafranceschi,¹⁵² M. Hohlmann,¹⁵² D. Noonan,¹⁵²
 M. Rahmani,¹⁵² T. Roy,¹⁵² F. Yumiceva,¹⁵² M. R. Adams,¹⁵³ L. Apanasevich,¹⁵³ D. Berry,¹⁵³ R. R. Betts,¹⁵³
 R. Cavanaugh,¹⁵³ X. Chen,¹⁵³ S. Dittmer,¹⁵³ O. Evdokimov,¹⁵³ C. E. Gerber,¹⁵³ D. A. Hangal,¹⁵³ D. J. Hofman,¹⁵³
 K. Jung,¹⁵³ J. Kamin,¹⁵³ C. Mills,¹⁵³ I. D. Sandoval Gonzalez,¹⁵³ M. B. Tonjes,¹⁵³ N. Varelas,¹⁵³ H. Wang,¹⁵³ X. Wang,¹⁵³
 Z. Wu,¹⁵³ J. Zhang,¹⁵³ M. Alhousseini,¹⁵⁴ B. Bilki,^{154,qqq} W. Clarida,¹⁵⁴ K. Dilsiz,^{154,rrr} S. Durgut,¹⁵⁴ R. P. Gandrajula,¹⁵⁴
 M. Haytmyradov,¹⁵⁴ V. Khristenko,¹⁵⁴ J.-P. Merlo,¹⁵⁴ A. Mestvirishvili,¹⁵⁴ A. Moeller,¹⁵⁴ J. Nachtman,¹⁵⁴ H. Ogul,^{154,sss}
 Y. Onel,¹⁵⁴ F. Ozok,^{154,ttt} A. Penzo,¹⁵⁴ C. Snyder,¹⁵⁴ E. Tiras,¹⁵⁴ J. Wetzel,¹⁵⁴ B. Blumenfeld,¹⁵⁵ A. Cocoros,¹⁵⁵
 N. Eminizer,¹⁵⁵ D. Fehling,¹⁵⁵ L. Feng,¹⁵⁵ A. V. Gritsan,¹⁵⁵ W. T. Hung,¹⁵⁵ P. Maksimovic,¹⁵⁵ J. Roskes,¹⁵⁵ U. Sarica,¹⁵⁵
 M. Swartz,¹⁵⁵ M. Xiao,¹⁵⁵ C. You,¹⁵⁵ A. Al-bataineh,¹⁵⁶ P. Baringer,¹⁵⁶ A. Bean,¹⁵⁶ S. Boren,¹⁵⁶ J. Bowen,¹⁵⁶ A. Bylinkin,¹⁵⁶
 J. Castle,¹⁵⁶ S. Khalil,¹⁵⁶ A. Kropivnitskaya,¹⁵⁶ D. Majumder,¹⁵⁶ W. Mcbrayer,¹⁵⁶ M. Murray,¹⁵⁶ C. Rogan,¹⁵⁶ S. Sanders,¹⁵⁶
 E. Schmitz,¹⁵⁶ J. D. Tapia Takaki,¹⁵⁶ Q. Wang,¹⁵⁶ S. Duric,¹⁵⁷ A. Ivanov,¹⁵⁷ K. Kaadze,¹⁵⁷ D. Kim,¹⁵⁷ Y. Maravin,¹⁵⁷

D. R. Mendis,¹⁵⁷ T. Mitchell,¹⁵⁷ A. Modak,¹⁵⁷ A. Mohammadi,¹⁵⁷ L. K. Saini,¹⁵⁷ N. Skhirtladze,¹⁵⁷ F. Rebassoo,¹⁵⁸ D. Wright,¹⁵⁸ A. Baden,¹⁵⁹ O. Baron,¹⁵⁹ A. Belloni,¹⁵⁹ S. C. Eno,¹⁵⁹ Y. Feng,¹⁵⁹ C. Ferraioli,¹⁵⁹ N. J. Hadley,¹⁵⁹ S. Jabeen,¹⁵⁹ G. Y. Jeng,¹⁵⁹ R. G. Kellogg,¹⁵⁹ J. Kunkle,¹⁵⁹ A. C. Mignerey,¹⁵⁹ F. Ricci-Tam,¹⁵⁹ Y. H. Shin,¹⁵⁹ A. Skuja,¹⁵⁹ S. C. Tonwar,¹⁵⁹ K. Wong,¹⁵⁹ D. Abercrombie,¹⁶⁰ B. Allen,¹⁶⁰ V. Azzolini,¹⁶⁰ A. Baty,¹⁶⁰ G. Bauer,¹⁶⁰ R. Bi,¹⁶⁰ S. Brandt,¹⁶⁰ W. Busza,¹⁶⁰ I. A. Cali,¹⁶⁰ M. D'Alfonso,¹⁶⁰ Z. Demiragli,¹⁶⁰ G. Gomez Ceballos,¹⁶⁰ M. Goncharov,¹⁶⁰ P. Harris,¹⁶⁰ D. Hsu,¹⁶⁰ M. Hu,¹⁶⁰ Y. Iiyama,¹⁶⁰ G. M. Innocenti,¹⁶⁰ M. Klute,¹⁶⁰ D. Kovalskyi,¹⁶⁰ Y.-J. Lee,¹⁶⁰ P. D. Luckey,¹⁶⁰ B. Maier,¹⁶⁰ A. C. Marini,¹⁶⁰ C. McGinn,¹⁶⁰ C. Mironov,¹⁶⁰ S. Narayanan,¹⁶⁰ X. Niu,¹⁶⁰ C. Paus,¹⁶⁰ C. Roland,¹⁶⁰ G. Roland,¹⁶⁰ G. S. F. Stephans,¹⁶⁰ K. Sumorok,¹⁶⁰ K. Tatar,¹⁶⁰ D. Velicanu,¹⁶⁰ J. Wang,¹⁶⁰ T. W. Wang,¹⁶⁰ B. Wyslouch,¹⁶⁰ S. Zhaozhong,¹⁶⁰ A. C. Benvenuti,¹⁶¹ R. M. Chatterjee,¹⁶¹ A. Evans,¹⁶¹ P. Hansen,¹⁶¹ S. Kalafut,¹⁶¹ Y. Kubota,¹⁶¹ Z. Lesko,¹⁶¹ J. Mans,¹⁶¹ N. Ruckstuhl,¹⁶¹ R. Rusack,¹⁶¹ J. Turkewitz,¹⁶¹ M. A. Wadud,¹⁶¹ J. G. Acosta,¹⁶² S. Oliveros,¹⁶² E. Avdeeva,¹⁶³ K. Bloom,¹⁶³ D. R. Claes,¹⁶³ C. Fangmeier,¹⁶³ F. Golf,¹⁶³ R. Gonzalez Suarez,¹⁶³ R. Kamalieddin,¹⁶³ I. Kravchenko,¹⁶³ J. Monroy,¹⁶³ J. E. Siado,¹⁶³ G. R. Snow,¹⁶³ B. Stieger,¹⁶³ A. Godshalk,¹⁶⁴ C. Harrington,¹⁶⁴ I. Iashvili,¹⁶⁴ A. Kharchilava,¹⁶⁴ C. Mclean,¹⁶⁴ D. Nguyen,¹⁶⁴ A. Parker,¹⁶⁴ S. Rappoccio,¹⁶⁴ B. Roozbahani,¹⁶⁴ G. Alverson,¹⁶⁵ E. Barberis,¹⁶⁵ C. Freer,¹⁶⁵ A. Hortiangtham,¹⁶⁵ D. M. Morse,¹⁶⁵ T. Orimoto,¹⁶⁵ R. Teixeira De Lima,¹⁶⁵ T. Wamorkar,¹⁶⁵ B. Wang,¹⁶⁵ A. Wisecarver,¹⁶⁵ D. Wood,¹⁶⁵ S. Bhattacharya,¹⁶⁶ O. Charaf,¹⁶⁶ K. A. Hahn,¹⁶⁶ N. Mucia,¹⁶⁶ N. Odell,¹⁶⁶ M. H. Schmitt,¹⁶⁶ K. Sung,¹⁶⁶ M. Trovato,¹⁶⁶ M. Velasco,¹⁶⁶ R. Bucci,¹⁶⁷ N. Dev,¹⁶⁷ M. Hildreth,¹⁶⁷ K. Hurtado Anampa,¹⁶⁷ C. Jessop,¹⁶⁷ D. J. Karmgard,¹⁶⁷ N. Kellams,¹⁶⁷ K. Lannon,¹⁶⁷ W. Li,¹⁶⁷ N. Loukas,¹⁶⁷ N. Marinelli,¹⁶⁷ F. Meng,¹⁶⁷ C. Mueller,¹⁶⁷ Y. Musienko,^{167,ii} M. Planer,¹⁶⁷ A. Reinsvold,¹⁶⁷ R. Ruchti,¹⁶⁷ P. Siddireddy,¹⁶⁷ G. Smith,¹⁶⁷ S. Taroni,¹⁶⁷ M. Wayne,¹⁶⁷ A. Wightman,¹⁶⁷ M. Wolf,¹⁶⁷ A. Woodard,¹⁶⁷ J. Alimena,¹⁶⁸ L. Antonelli,¹⁶⁸ B. Bylsma,¹⁶⁸ L. S. Durkin,¹⁶⁸ S. Flowers,¹⁶⁸ B. Francis,¹⁶⁸ A. Hart,¹⁶⁸ C. Hill,¹⁶⁸ W. Ji,¹⁶⁸ T. Y. Ling,¹⁶⁸ W. Luo,¹⁶⁸ B. L. Winer,¹⁶⁸ H. W. Wulsin,¹⁶⁸ S. Cooperstein,¹⁶⁹ P. Elmer,¹⁶⁹ J. Hardenbrook,¹⁶⁹ S. Higginbotham,¹⁶⁹ A. Kalogeropoulos,¹⁶⁹ D. Lange,¹⁶⁹ M. T. Lucchini,¹⁶⁹ J. Luo,¹⁶⁹ D. Marlow,¹⁶⁹ K. Mei,¹⁶⁹ I. Ojalvo,¹⁶⁹ J. Olsen,¹⁶⁹ C. Palmer,¹⁶⁹ P. Piroué,¹⁶⁹ J. Salfeld-Nebgen,¹⁶⁹ D. Stickland,¹⁶⁹ C. Tully,¹⁶⁹ S. Malik,¹⁷⁰ S. Norberg,¹⁷⁰ A. Barker,¹⁷¹ V. E. Barnes,¹⁷¹ S. Das,¹⁷¹ L. Gutay,¹⁷¹ M. Jones,¹⁷¹ A. W. Jung,¹⁷¹ A. Khatiwada,¹⁷¹ B. Mahakud,¹⁷¹ D. H. Miller,¹⁷¹ N. Neumeister,¹⁷¹ C. C. Peng,¹⁷¹ S. Piperov,¹⁷¹ H. Qiu,¹⁷¹ J. F. Schulte,¹⁷¹ J. Sun,¹⁷¹ F. Wang,¹⁷¹ R. Xiao,¹⁷¹ W. Xie,¹⁷¹ T. Cheng,¹⁷² J. Dolen,¹⁷² N. Parashar,¹⁷² Z. Chen,¹⁷³ K. M. Ecklund,¹⁷³ S. Freed,¹⁷³ F. J. M. Geurts,¹⁷³ M. Kilpatrick,¹⁷³ W. Li,¹⁷³ B. P. Padley,¹⁷³ J. Roberts,¹⁷³ J. Rorie,¹⁷³ W. Shi,¹⁷³ Z. Tu,¹⁷³ J. Zabel,¹⁷³ A. Zhang,¹⁷³ A. Bodek,¹⁷⁴ P. de Barbaro,¹⁷⁴ R. Demina,¹⁷⁴ Y. t. Duh,¹⁷⁴ J. L. Dulemba,¹⁷⁴ C. Fallon,¹⁷⁴ T. Ferbel,¹⁷⁴ M. Galanti,¹⁷⁴ A. Garcia-Bellido,¹⁷⁴ J. Han,¹⁷⁴ O. Hindrichs,¹⁷⁴ A. Khukhunaishvili,¹⁷⁴ P. Tan,¹⁷⁴ R. Taus,¹⁷⁴ A. Agapitos,¹⁷⁵ J. P. Chou,¹⁷⁵ Y. Gershtein,¹⁷⁵ E. Halkiadakis,¹⁷⁵ M. Heindl,¹⁷⁵ E. Hughes,¹⁷⁵ S. Kaplan,¹⁷⁵ R. Kunnawalkam Elayavalli,¹⁷⁵ S. Kyriacou,¹⁷⁵ A. Lath,¹⁷⁵ R. Montalvo,¹⁷⁵ K. Nash,¹⁷⁵ M. Osherson,¹⁷⁵ H. Saka,¹⁷⁵ S. Salur,¹⁷⁵ S. Schnetzer,¹⁷⁵ D. Sheffield,¹⁷⁵ S. Somalwar,¹⁷⁵ R. Stone,¹⁷⁵ S. Thomas,¹⁷⁵ P. Thomassen,¹⁷⁵ M. Walker,¹⁷⁵ A. G. Delannoy,¹⁷⁶ J. Heideman,¹⁷⁶ G. Riley,¹⁷⁶ S. Spanier,¹⁷⁶ O. Bouhali,^{177,uuu} A. Celik,¹⁷⁷ M. Dalchenko,¹⁷⁷ M. De Mattia,¹⁷⁷ A. Delgado,¹⁷⁷ S. Dildick,¹⁷⁷ R. Eusebi,¹⁷⁷ J. Gilmore,¹⁷⁷ T. Huang,¹⁷⁷ T. Kamon,^{177,vvv} S. Luo,¹⁷⁷ R. Mueller,¹⁷⁷ A. Perloff,¹⁷⁷ L. Perniè,¹⁷⁷ D. Rathjens,¹⁷⁷ A. Safonov,¹⁷⁷ N. Akchurin,¹⁷⁸ J. Damgov,¹⁷⁸ F. De Guio,¹⁷⁸ P. R. Duerdo,¹⁷⁸ S. Kunori,¹⁷⁸ K. Lamichhane,¹⁷⁸ S. W. Lee,¹⁷⁸ T. Mengke,¹⁷⁸ S. Muthumuni,¹⁷⁸ T. Peltola,¹⁷⁸ S. Undleeb,¹⁷⁸ I. Volobouev,¹⁷⁸ Z. Wang,¹⁷⁸ S. Greene,¹⁷⁹ A. Gurrola,¹⁷⁹ R. Janjam,¹⁷⁹ W. Johns,¹⁷⁹ C. Maguire,¹⁷⁹ A. Melo,¹⁷⁹ H. Ni,¹⁷⁹ K. Padeken,¹⁷⁹ J. D. Ruiz Alvarez,¹⁷⁹ P. Sheldon,¹⁷⁹ S. Tuo,¹⁷⁹ J. Velkovska,¹⁷⁹ M. Verweij,¹⁷⁹ Q. Xu,¹⁷⁹ M. W. Arenton,¹⁸⁰ P. Barria,¹⁸⁰ B. Cox,¹⁸⁰ R. Hirosky,¹⁸⁰ M. Joyce,¹⁸⁰ A. Ledovskoy,¹⁸⁰ H. Li,¹⁸⁰ C. Neu,¹⁸⁰ T. Sinthuprasith,¹⁸⁰ Y. Wang,¹⁸⁰ E. Wolfe,¹⁸⁰ F. Xia,¹⁸⁰ R. Harr,¹⁸¹ P. E. Karchin,¹⁸¹ N. Poudyal,¹⁸¹ J. Sturdy,¹⁸¹ P. Thapa,¹⁸¹ S. Zaleski,¹⁸¹ M. Brodski,¹⁸² J. Buchanan,¹⁸² C. Caillol,¹⁸² D. Carlsmith,¹⁸² S. Dasu,¹⁸² L. Dodd,¹⁸² B. Gombert,¹⁸² M. Grothe,¹⁸² M. Herndon,¹⁸² A. Hervé,¹⁸² U. Hussain,¹⁸² P. Klabbers,¹⁸² A. Lanaro,¹⁸² K. Long,¹⁸² R. Loveless,¹⁸² T. Ruggles,¹⁸² A. Savin,¹⁸² N. Smith,¹⁸² W. H. Smith,¹⁸² and N. Woods¹⁸²

(CMS Collaboration)

¹Yerevan Physics Institute, Yerevan, Armenia²Institut für Hochenergiephysik, Wien, Austria³Institute for Nuclear Problems, Minsk, Belarus⁴Universiteit Antwerpen, Antwerpen, Belgium⁵Vrije Universiteit Brussel, Brussel, Belgium

- ⁶*Université Libre de Bruxelles, Bruxelles, Belgium*
⁷*Ghent University, Ghent, Belgium*
⁸*Université Catholique de Louvain, Louvain-la-Neuve, Belgium*
⁹*Centro Brasileiro de Pesquisas Físicas, Rio de Janeiro, Brazil*
¹⁰*Universidade do Estado do Rio de Janeiro, Rio de Janeiro, Brazil*
^{11a}*Universidade Estadual Paulista, São Paulo, Brazil*
^{11b}*Universidade Federal do ABC, São Paulo, Brazil*
¹²*Institute for Nuclear Research and Nuclear Energy, Bulgarian Academy of Sciences, Sofia, Bulgaria*
¹³*University of Sofia, Sofia, Bulgaria*
¹⁴*Beihang University, Beijing, China*
¹⁵*Institute of High Energy Physics, Beijing, China*
¹⁶*State Key Laboratory of Nuclear Physics and Technology, Peking University, Beijing, China*
¹⁷*Tsinghua University, Beijing, China*
¹⁸*Universidad de Los Andes, Bogota, Colombia*
¹⁹*University of Split, Faculty of Electrical Engineering, Mechanical Engineering and Naval Architecture, Split, Croatia*
²⁰*University of Split, Faculty of Science, Split, Croatia*
²¹*Institute Rudjer Boskovic, Zagreb, Croatia*
²²*University of Cyprus, Nicosia, Cyprus*
²³*Charles University, Prague, Czech Republic*
²⁴*Escuela Politécnica Nacional, Quito, Ecuador*
²⁵*Universidad San Francisco de Quito, Quito, Ecuador*
²⁶*Academy of Scientific Research and Technology of the Arab Republic of Egypt, Egyptian Network of High Energy Physics, Cairo, Egypt*
²⁷*National Institute of Chemical Physics and Biophysics, Tallinn, Estonia*
²⁸*Department of Physics, University of Helsinki, Helsinki, Finland*
²⁹*Helsinki Institute of Physics, Helsinki, Finland*
³⁰*Lappeenranta University of Technology, Lappeenranta, Finland*
³¹*IRFU, CEA, Université Paris-Saclay, Gif-sur-Yvette, France*
³²*Laboratoire Leprince-Ringuet, Ecole polytechnique, CNRS/IN2P3, Université Paris-Saclay, Palaiseau, France*
³³*Université de Strasbourg, CNRS, IPHC UMR 7178, Strasbourg, France*
³⁴*Centre de Calcul de l'Institut National de Physique Nucléaire et de Physique des Particules, CNRS/IN2P3, Villeurbanne, France*
³⁵*Université de Lyon, Université Claude Bernard Lyon 1, CNRS-IN2P3, Institut de Physique Nucléaire de Lyon, Villeurbanne, France*
³⁶*Georgian Technical University, Tbilisi, Georgia*
³⁷*Tbilisi State University, Tbilisi, Georgia*
³⁸*RWTH Aachen University, I. Physikalisches Institut, Aachen, Germany*
³⁹*RWTH Aachen University, III. Physikalisches Institut A, Aachen, Germany*
⁴⁰*RWTH Aachen University, III. Physikalisches Institut B, Aachen, Germany*
⁴¹*Deutsches Elektronen-Synchrotron, Hamburg, Germany*
⁴²*University of Hamburg, Hamburg, Germany*
⁴³*Karlsruher Institut fuer Technology*
⁴⁴*Institute of Nuclear and Particle Physics (INPP), NCSR Demokritos, Aghia Paraskevi, Greece*
⁴⁵*National and Kapodistrian University of Athens, Athens, Greece*
⁴⁶*National Technical University of Athens, Athens, Greece*
⁴⁷*University of Ioánnina, Ioánnina, Greece*
⁴⁸*MTA-ELTE Lendület CMS Particle and Nuclear Physics Group, Eötvös Loránd University, Budapest, Hungary*
⁴⁹*Wigner Research Centre for Physics, Budapest, Hungary*
⁵⁰*Institute of Nuclear Research ATOMKI, Debrecen, Hungary*
⁵¹*Institute of Physics, University of Debrecen, Debrecen, Hungary*
⁵²*Indian Institute of Science (IISc), Bangalore, India*
⁵³*National Institute of Science Education and Research, HBNI, Bhubaneswar, India*
⁵⁴*Panjab University, Chandigarh, India*
⁵⁵*University of Delhi, Delhi, India*
⁵⁶*Saha Institute of Nuclear Physics, HBNI, Kolkata, India*
⁵⁷*Indian Institute of Technology Madras, Madras, India*
⁵⁸*Bhabha Atomic Research Centre, Mumbai, India*

- ⁵⁹*Tata Institute of Fundamental Research-A, Mumbai, India*
⁶⁰*Tata Institute of Fundamental Research-B, Mumbai, India*
⁶¹*Indian Institute of Science Education and Research (IISER), Pune, India*
⁶²*Institute for Research in Fundamental Sciences (IPM), Tehran, Iran*
⁶³*University College Dublin, Dublin, Ireland*
^{64a}*INFN Sezione di Bari, Bari, Italy*
^{64b}*Università di Bari, Bari, Italy*
^{64c}*Politecnico di Bari, Bari, Italy*
^{65a}*INFN Sezione di Bologna, Bologna, Italy*
^{65b}*Università di Bologna, Bologna, Italy*
^{66a}*INFN Sezione di Catania, Catania, Italy*
^{66b}*Università di Catania, Catania, Italy*
^{67a}*INFN Sezione di Firenze, Firenze, Italy*
^{67b}*Università di Firenze, Firenze, Italy*
⁶⁸*INFN Laboratori Nazionali di Frascati, Frascati, Italy*
^{69a}*INFN Sezione di Genova, Genova, Italy*
^{69b}*Università di Genova, Genova, Italy*
^{70a}*INFN Sezione di Milano-Bicocca, Milano, Italy*
^{70b}*Università di Milano-Bicocca, Milano, Italy*
^{71a}*INFN Sezione di Napoli, Roma, Italy*
^{71b}*Università di Napoli 'Federico II', Roma, Italy*
^{71c}*Università della Basilicata, Roma, Italy*
^{71d}*Università G. Marconi, Roma, Italy*
^{72a}*INFN Sezione di Padova, Trento, Italy*
^{72b}*Università di Padova, Trento, Italy*
^{73a}*INFN Sezione di Pavia*
^{73b}*Università di Pavia*
^{74a}*INFN Sezione di Perugia, Perugia, Italy*
^{74b}*Università di Perugia, Perugia, Italy*
^{75a}*INFN Sezione di Pisa, Pisa, Italy*
^{75b}*Università di Pisa, Pisa, Italy*
^{75c}*Scuola Normale Superiore di Pisa, Pisa, Italy*
^{76a}*INFN Sezione di Roma, Rome, Italy*
^{76b}*Sapienza Università di Roma, Rome, Italy*
^{77a}*INFN Sezione di Torino, Novara, Italy*
^{77b}*Università di Torino, Novara, Italy*
^{77c}*Università del Piemonte Orientale, Novara, Italy*
^{78a}*INFN Sezione di Trieste, Trieste, Italy*
^{78b}*Università di Trieste, Trieste, Italy*
⁷⁹*Kyungpook National University*
⁸⁰*Chonnam National University, Institute for Universe and Elementary Particles, Kwangju, Korea*
⁸¹*Hanyang University, Seoul, Korea*
⁸²*Korea University, Seoul, Korea*
⁸³*Sejong University, Seoul, Korea*
⁸⁴*Seoul National University, Seoul, Korea*
⁸⁵*University of Seoul, Seoul, Korea*
⁸⁶*Sungkyunkwan University, Suwon, Korea*
⁸⁷*Vilnius University, Vilnius, Lithuania*
⁸⁸*National Centre for Particle Physics, Universiti Malaya, Kuala Lumpur, Malaysia*
⁸⁹*Universidad de Sonora (UNISON), Hermosillo, Mexico*
⁹⁰*Centro de Investigacion y de Estudios Avanzados del IPN, Mexico City, Mexico*
⁹¹*Universidad Iberoamericana, Mexico City, Mexico*
⁹²*Benemerita Universidad Autonoma de Puebla, Puebla, Mexico*
⁹³*Universidad Autónoma de San Luis Potosí, San Luis Potosí, Mexico*
⁹⁴*University of Auckland, Auckland, New Zealand*
⁹⁵*University of Canterbury, Christchurch, New Zealand*
⁹⁶*National Centre for Physics, Quaid-I-Azam University, Islamabad, Pakistan*
⁹⁷*National Centre for Nuclear Research, Swierk, Poland*
⁹⁸*Institute of Experimental Physics, Faculty of Physics, University of Warsaw, Warsaw, Poland*
⁹⁹*Laboratório de Instrumentação e Física Experimental de Partículas, Lisboa, Portugal*

- ¹⁰⁰*Joint Institute for Nuclear Research, Dubna, Russia*
- ¹⁰¹*Petersburg Nuclear Physics Institute, Gatchina (St. Petersburg), Russia*
- ¹⁰²*Institute for Nuclear Research, Moscow, Russia*
- ¹⁰³*Institute for Theoretical and Experimental Physics, Moscow, Russia*
- ¹⁰⁴*Moscow Institute of Physics and Technology, Moscow, Russia*
- ¹⁰⁵*National Research Nuclear University 'Moscow Engineering Physics Institute' (MEPhI), Moscow, Russia*
- ¹⁰⁶*P.N. Lebedev Physical Institute, Moscow, Russia*
- ¹⁰⁷*Skobeltsyn Institute of Nuclear Physics, Lomonosov Moscow State University, Moscow, Russia*
- ¹⁰⁸*Novosibirsk State University (NSU), Novosibirsk, Russia*
- ¹⁰⁹*State Research Center of Russian Federation, Institute for High Energy Physics of NRC "Kurchatov Institute", Protvino, Russia*
- ¹¹⁰*National Research Tomsk Polytechnic University, Tomsk, Russia*
- ¹¹¹*University of Belgrade, Faculty of Physics and Vinca Institute of Nuclear Sciences, Belgrade, Serbia*
- ¹¹²*Centro de Investigaciones Energéticas Medioambientales y Tecnológicas (CIEMAT), Madrid, Spain*
- ¹¹³*Universidad Autónoma de Madrid, Madrid, Spain*
- ¹¹⁴*Universidad de Oviedo, Oviedo, Spain*
- ¹¹⁵*Instituto de Física de Cantabria (IFCA), CSIC-Universidad de Cantabria, Santander, Spain*
- ¹¹⁶*University of Ruhuna, Department of Physics, Matara, Sri Lanka*
- ¹¹⁷*CERN, European Organization for Nuclear Research, Geneva, Switzerland*
- ¹¹⁸*Paul Scherrer Institut, Villigen, Switzerland*
- ¹¹⁹*ETH Zurich—Institute for Particle Physics and Astrophysics (IPA), Zurich, Switzerland*
- ¹²⁰*Universität Zürich, Zurich, Switzerland*
- ¹²¹*National Central University, Chung-Li, Taiwan*
- ¹²²*National Taiwan University (NTU), Taipei, Taiwan*
- ¹²³*Chulalongkorn University, Faculty of Science, Department of Physics, Bangkok, Thailand*
- ¹²⁴*Çukurova University, Physics Department, Science and Art Faculty, Adana, Turkey*
- ¹²⁵*Middle East Technical University, Physics Department, Ankara, Turkey*
- ¹²⁶*Bogazici University, Istanbul, Turkey*
- ¹²⁷*Istanbul Technical University, Istanbul, Turkey*
- ¹²⁸*Institute for Scintillation Materials of National Academy of Science of Ukraine, Kharkov, Ukraine*
- ¹²⁹*National Scientific Center, Kharkov Institute of Physics and Technology, Kharkov, Ukraine*
- ¹³⁰*University of Bristol, Bristol, United Kingdom*
- ¹³¹*Rutherford Appleton Laboratory, Didcot, United Kingdom*
- ¹³²*Imperial College, London, United Kingdom*
- ¹³³*Brunel University, Uxbridge, United Kingdom*
- ¹³⁴*Baylor University, Waco, Texas, USA*
- ¹³⁵*Catholic University of America, Washington, DC, USA*
- ¹³⁶*The University of Alabama, Tuscaloosa, Alabama, USA*
- ¹³⁷*Boston University, Boston, Massachusetts, USA*
- ¹³⁸*Brown University, Providence, Rhode Island, USA*
- ¹³⁹*University of California, Davis, Davis, California, USA*
- ¹⁴⁰*University of California, Los Angeles, California, USA*
- ¹⁴¹*University of California, Riverside, Riverside, California, USA*
- ¹⁴²*University of California, San Diego, La Jolla, California, USA*
- ¹⁴³*University of California, Santa Barbara—Department of Physics, Santa Barbara, California, USA*
- ¹⁴⁴*California Institute of Technology, Pasadena, California, USA*
- ¹⁴⁵*Carnegie Mellon University, Pittsburgh, Pennsylvania, USA*
- ¹⁴⁶*University of Colorado Boulder, Boulder, Colorado, USA*
- ¹⁴⁷*Cornell University, Ithaca, New York, USA*
- ¹⁴⁸*Fermi National Accelerator Laboratory, Batavia, Illinois, USA*
- ¹⁴⁹*University of Florida, Gainesville, Florida, USA*
- ¹⁵⁰*Florida International University, Miami, Florida, USA*
- ¹⁵¹*Florida State University, Tallahassee, Florida, USA*
- ¹⁵²*Florida Institute of Technology, Melbourne, Florida, USA*
- ¹⁵³*University of Illinois at Chicago (UIC), Chicago, Illinois, USA*
- ¹⁵⁴*The University of Iowa, Iowa City, Iowa, USA*
- ¹⁵⁵*Johns Hopkins University, Baltimore, Maryland, USA*
- ¹⁵⁶*The University of Kansas, Lawrence, Kansas, USA*
- ¹⁵⁷*Kansas State University, Manhattan, Kansas, USA*

- ¹⁵⁸*Lawrence Livermore National Laboratory, Livermore, California, USA*
¹⁵⁹*University of Maryland, College Park, Maryland, USA*
¹⁶⁰*Massachusetts Institute of Technology, Cambridge, Massachusetts, USA*
¹⁶¹*University of Minnesota, Minneapolis, Minnesota, USA*
¹⁶²*University of Mississippi, Oxford, Mississippi, USA*
¹⁶³*University of Nebraska-Lincoln, Lincoln, Nebraska, USA*
¹⁶⁴*State University of New York, Buffalo, Buffalo, New York, USA*
¹⁶⁵*Northeastern University, Boston, Massachusetts, USA*
¹⁶⁶*Northwestern University, Evanston, Illinois, USA*
¹⁶⁷*University of Notre Dame, Notre Dame, Indiana, USA*
¹⁶⁸*The Ohio State University, Columbus, Ohio, USA*
¹⁶⁹*Princeton University, Princeton, New Jersey, USA*
¹⁷⁰*University of Puerto Rico, Mayaguez, Puerto Rico*
¹⁷¹*Purdue University, West Lafayette, Indiana, USA*
¹⁷²*Purdue University Northwest, Hammond, Indiana, USA*
¹⁷³*Rice University, Houston, Texas, USA*
¹⁷⁴*University of Rochester, Rochester, New York, USA*
¹⁷⁵*Rutgers, The State University of New Jersey, Piscataway, New Jersey, USA*
¹⁷⁶*University of Tennessee, Knoxville, Tennessee, USA*
¹⁷⁷*Texas A&M University, College Station, Texas, USA*
¹⁷⁸*Texas Tech University, Lubbock, Texas, USA*
¹⁷⁹*Vanderbilt University, Nashville, Tennessee, USA*
¹⁸⁰*University of Virginia, Charlottesville, Virginia, USA*
¹⁸¹*Wayne State University, Detroit, Michigan, USA*
¹⁸²*University of Wisconsin—Madison, Madison, Wisconsin, USA*

^aDeceased.

^bAlso at Vienna University of Technology, Vienna, Austria.

^cAlso at IRFU, CEA, Université Paris-Saclay, Gif-sur-Yvette, France.

^dAlso at Universidade Estadual de Campinas, Campinas, Brazil.

^eAlso at Federal University of Rio Grande do Sul, Porto Alegre, Brazil.

^fAlso at Université Libre de Bruxelles, Bruxelles, Belgium.

^gAlso at University of Chinese Academy of Sciences.

^hAlso at Institute for Theoretical and Experimental Physics, Moscow, Russia.

ⁱAlso at Joint Institute for Nuclear Research, Dubna, Russia.

^jAlso at British University in Egypt, Cairo, Egypt.

^kAlso at Suez University, Suez, Egypt.

^lAlso at Zewail City of Science and Technology, Zewail, Egypt.

^mAlso at Department of Physics, King Abdulaziz University, Jeddah, Saudi Arabia.

ⁿAlso at Université de Haute Alsace, Mulhouse, France.

^oAlso at Skobeltsyn Institute of Nuclear Physics, Lomonosov Moscow State University, Moscow, Russia.

^pAlso at CERN, European Organization for Nuclear Research, Geneva, Switzerland.

^qAlso at RWTH Aachen University, III. Physikalisches Institut A, Aachen, Germany.

^rAlso at University of Hamburg, Hamburg, Germany.

^sAlso at Brandenburg University of Technology, Cottbus, Germany.

^tAlso at MTA-ELTE Lendület CMS Particle and Nuclear Physics Group, Eötvös Loránd University, Budapest, Hungary.

^uAlso at Institute of Nuclear Research ATOMKI, Debrecen, Hungary.

^vAlso at Institute of Physics, University of Debrecen, Debrecen, Hungary.

^wAlso at IIT Bhubaneswar, Bhubaneswar, India.

^xAlso at Institute of Physics, Bhubaneswar, India.

^yAlso at Shoolini University, Solan, India.

^zAlso at University of Visva-Bharati, Santiniketan, India.

^{aa}Also at Isfahan University of Technology, Isfahan, Iran.

^{bb}Also at Plasma Physics Research Center, Science and Research Branch, Islamic Azad University, Tehran, Iran.

^{cc}Also at Università degli Studi di Siena, Siena, Italy.

^{dd}Also at Kyunghee University, Seoul, Korea.

^{ee}Also at International Islamic University of Malaysia, Kuala Lumpur, Malaysia.

^{ff}Also at Malaysian Nuclear Agency, MOSTI, Kajang, Malaysia.

^{gg}Also at Consejo Nacional de Ciencia y Tecnología, Mexico city, Mexico.

^{hh}Also at Warsaw University of Technology, Institute of Electronic Systems, Warsaw, Poland.

- ii Also at Institute for Nuclear Research, Moscow, Russia.
- jj Also at National Research Nuclear University 'Moscow Engineering Physics Institute' (MEPhI), Moscow, Russia.
- kk Also at St. Petersburg State Polytechnical University, St. Petersburg, Russia.
- ll Also at University of Florida, Gainesville, Florida, USA.
- mm Also at P.N. Lebedev Physical Institute, Moscow, Russia.
- nn Also at California Institute of Technology, Pasadena, California, USA.
- oo Also at Budker Institute of Nuclear Physics, Novosibirsk, Russia.
- pp Also at Faculty of Physics, University of Belgrade, Belgrade, Serbia.
- qq Also at INFN Sezione di Pavia, Università di Pavia, Pavia, Italy.
- rr Also at University of Belgrade, Faculty of Physics and Vinca Institute of Nuclear Sciences, Belgrade, Serbia.
- ss Also at Scuola Normale e Sezione dell'INFN, Pisa, Italy.
- tt Also at National and Kapodistrian University of Athens, Athens, Greece.
- uu Also at Riga Technical University.
- vv Also at Universität Zürich, Zurich, Switzerland.
- ww Also at Stefan Meyer Institute for Subatomic Physics.
- xx Also at Adiyaman University, Adiyaman, Turkey.
- yy Also at Istanbul Aydin University, Istanbul, Turkey.
- zz Also at Mersin University, Mersin, Turkey.
- aaa Also at Piri Reis University, Istanbul, Turkey.
- bbb Also at Gaziosmanpasa University, Tokat, Turkey.
- ccc Also at Ozyegin University, Istanbul, Turkey.
- ddd Also at Izmir Institute of Technology, Izmir, Turkey.
- eee Also at Marmara University, Istanbul, Turkey.
- fff Also at Kafkas University, Kars, Turkey.
- ggg Also at Istanbul University, Faculty of Science, Istanbul, Turkey.
- hhh Also at Istanbul Bilgi University, Istanbul, Turkey.
- iii Also at Hacettepe University, Ankara, Turkey.
- jjj Also at Rutherford Appleton Laboratory, Didcot, United Kingdom.
- kkk Also at School of Physics and Astronomy, University of Southampton, Southampton, United Kingdom.
- lll Also at Monash University, Faculty of Science, Clayton, Australia.
- mmm Also at Bethel University.
- nnn Also at Karamanoğlu Mehmetbey University, Karaman, Turkey.
- ooo Also at Utah Valley University, Orem, Utah, USA.
- ppp Also at Purdue University, West Lafayette, Indiana, USA.
- qqq Also at Beykent University.
- rrr Also at Bingol University, Bingol, Turkey.
- sss Also at Sinop University, Sinop, Turkey.
- ttt Also at Mimar Sinan University, Istanbul, Istanbul, Turkey.
- uuu Also at Texas A&M University at Qatar, Doha, Qatar.
- vvv Also at Kyungpook National University.